Sensitivity in the Overland Reintensification of Tropical Cyclone Erin (2007) to Near-Surface Soil Moisture Characteristics

CLARK EVANS*

National Center for Atmospheric Research,[+] Boulder, Colorado

RUSS S. SCHUMACHER[#]

Department of Atmospheric Sciences, Texas A&M University, College Station, Texas

THOMAS J. GALARNEAU JR.[@]

Department of Atmospheric and Environmental Sciences, University at Albany, State University of New York, Albany, New York

(Manuscript received 13 August 2010, in final form 13 June 2011)

ABSTRACT

This study investigates the impact of abnormally moist soil conditions across the southern Great Plains upon the overland reintensification of North Atlantic Tropical Cyclone Erin (2007). This is tested by analyzing the contributions of three soil moisture–related signals—a seasonal signal, an along-track rainfall signal, and an early postlandfall rainfall signal—to the intensity of the vortex. In so doing, a suite of nine convection-permitting numerical simulations using the Advanced Research Weather Research and Forecasting model (WRF-ARW) is used. Of the signals tested, soil moisture contributions from the anomalously wet months preceding Erin are found to have the greatest positive impact upon the intensity of the vortex, though this impact is on the order of that from climatological soil moisture conditions. The greatest impact of the early rainfall signal contributions is found when it is added to the seasonal signal. Along-track rainfall during the simulation period has a minimal impact.

Variations in soil moisture content result in impacts upon the boundary layer thermodynamic environment via boundary layer mixing. Greater soil moisture content results in weaker mixing, a shallower boundary layer, and greater moisture and instability. Differences in the intensity of convection that develops and its accompanying latent heat release aloft result in greater warm-core development and surface vortex intensification within the simulations featuring greater soil moisture content. Implications of these findings to the tropical cyclone development process are discussed. Given that the reintensification is shown to occur in, apart from land, an otherwise favorable environment for tropical cyclone development and results in a vortex with a structure similar to developing tropical cyclones, these findings provide new insight into the conditions under which tropical cyclones develop.

1. Introduction

During the early morning hours of 19 August 2007, 3 days after making landfall as a tropical depression on the central Texas coastline, the remnant circulation associated with North Atlantic Tropical Cyclone (TC) Erin dramatically reintensified over west-central Oklahoma. Associated with this reintensification were a decrease in minimum sea level pressure from 1007 to 995 hPa and an increase in maximum sustained surface wind speed from 20 to 50 kt (~10 to ~25 m s^{-1}; Brennan et al. 2009). Noteworthy among these values is a lower minimum sea level pressure and greater maximum sustained surface wind speed than those observed while TC Erin (2007) was

* Current affiliation: Atmospheric Science Group, Department of Mathematical Sciences, University of Wisconsin—Milwaukee, Milwaukee, Wisconsin.

[+] The National Center for Atmospheric Research is sponsored by the National Science Foundation.

[#] Current affiliation: Department of Atmospheric Science, Colorado State University, Fort Collins, Colorado.

[@] Current affiliation: National Center for Atmospheric Research, Boulder, Colorado.

Corresponding author address: Dr. Clark Evans, Dept. of Mathematical Sciences, University of Wisconsin–Milwaukee, P. O. Box 413, Milwaukee, WI 53201-0413.
E-mail: a.clark.evans@gmail.com

DOI: 10.1175/2011MWR3593.1

at peak intensity over the open waters of the Gulf of Mexico. The reintensification of the remnant TC also brought about the development of an eyelike feature in the Weather Surveillance Radar-1988 Doppler (WSR-88D) imagery over west-central Oklahoma early on 19 August [Fig. 8d of Arndt et al. (2009)]. The life cycle of TC Erin is discussed by Brennan et al. (2009), meteorological observations during the reintensification period are detailed by Arndt et al. (2009), an analysis of the reintensifying cyclone and its environment is given by Monteverdi and Edwards (2010), and the far-reaching impacts of the remnant TC are discussed by Galarneau et al. (2010).

The occurrence of tropical storm-force winds associated with a TC over Oklahoma is not an unprecedented event. As noted by Arndt et al. (2009), five other TCs have brought tropical storm-force winds to Oklahoma. In contrast to these cases, however, TC Erin (2007) was in the process of intensifying to peak intensity over Oklahoma rather than dissipating. Furthermore, the overland reintensification of a TC, while rare, is also not an unprecedented event. The studies of Bosart and Lackmann (1995) and Bassill and Morgan (2006) documented the synoptic-scale environments associated with the overland reintensifications of TC David (1979) and TC Danny (1997), respectively, across the mid-Atlantic portion of the United States. Both studies highlighted the importance of a moist neutral thermodynamic profile in a weakly baroclinic environment to the observed overland TC reintensification. Moist neutral conditions help mitigate the development of deep cold pools and promote lower-tropospheric convergence, deep rising motion, and near-surface cyclonic vertical vorticity generation. Tropical Cyclone Erin is unique from these events in that it reintensified over the southern Great Plains rather than the mid-Atlantic states; however, the potential impact (if any) of this geographical difference upon the reintensification process is unclear.

Another means by which a remnant TC or TC-like vortex can reintensify over land is described by Emanuel et al. (2008) in a study of TC reintensification over the deserts of Australia. This overland reintensification mechanism, operating on time scales of hours to days, is driven by enhanced surface latent heat fluxes (e.g., Rotunno and Emanuel 1987). Rainfall along and ahead of the track of a TC over land contributes to increased soil moisture content of the sandy soils of the Australian desert. Such desert soils are excellent natural heat and moisture conductors. Daytime heating ahead of the TC warms these soils, contributing to latent heat fluxes sufficiently large so as to allow for vortex reintensification over land in an otherwise favorable environment for TC development (e.g., Emanuel et al. 2008; Montgomery et al. 2009). Subsequent vortex decay occurs after

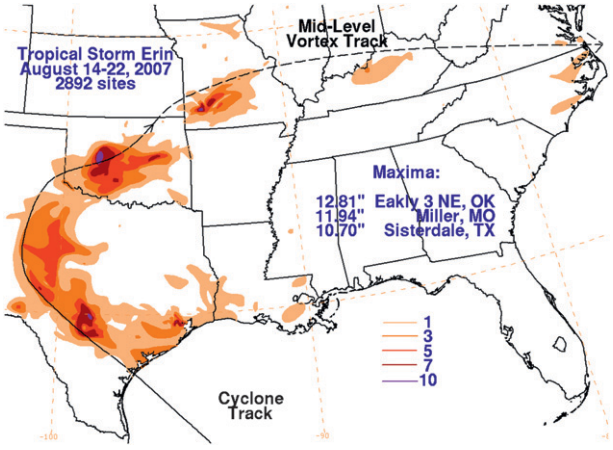

FIG. 1. Observed rainfall (shaded; units: in.) during 14–22 Aug 2007 associated with TC Erin (2007). The track of the vortex is depicted by the solid black line. (Image obtained from http://www.hpc.ncep.noaa.gov/tropical/rain/erin2007filledrainwhite.gif.)

environmental moisture transport that supports the soil-moistening rains is weakened or eliminated. Support for this hypothesis is provided by a number of studies on the response of TC-like vortices to wetter or more waterlike surface conditions (e.g., Shen et al. 2002; Tuleya 1994).

In a conference presentation, Emanuel (2008) extended this theory to TC Erin (2007), hypothesizing that a similar mechanism operating on longer time scales may be responsible for the overland reintensification of TC Erin. Enhanced rainfall during the anomalously wet March–July 2007 period, as noted by Arndt et al. (2009), resulted in relatively moist soils (cf. climatology) along and to the right of the track of the remnant TC. Additionally, the thermal conductivity characteristics of the somewhat sandy soils of western Oklahoma (e.g., Emanuel 2008, slide 29) are similar to but slightly lower than those of the deserts of Australia [e.g., Fig. 5 of Geo4Va (2011)]. This suggests that strong heating of these soils ahead of the remnant TC, as described by Emanuel et al. (2008), may allow for the generation of enhanced surface heat and moisture fluxes in the remnant TC's environment. From this, Emanuel (2008) posed that TC Erin (2007) experienced a TC-like reintensification early on 19 August 2007 as it passed over the resultant region of enhanced latent heat fluxes, subsequently decaying as it moved eastward away from the region of sandy soils and greater soil moisture content.

The works of Emanuel et al. (2008) and Emanuel (2008) each highlight how soil moisture content and accompanying land surface feedbacks on multiple time scales may increase the intensity of TC Erin (2007). These are hereafter referred to as the ''TC rainfall'' and ''seasonal'' signals, respectively. In addition, very heavy rainfall associated with TC Erin on 16–17 August 2007 across central Texas (e.g., Fig. 1) moistened soils under

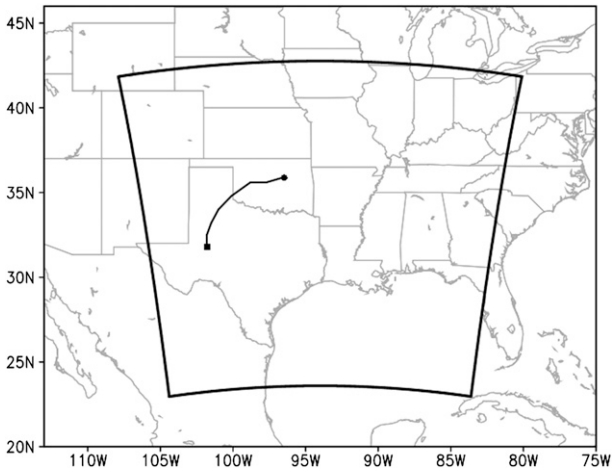

FIG. 2. Simulation domain employed within the WRF-ARW v3.1 model simulations carried out in this study. The observed track of TC Erin (2007) is depicted by the solid black line.

TABLE 1. Model configuration utilized within the control simulation of TC Erin (2007).

Model parameter	Selected configuration
Model version	WRF-ARW v3.1 (Skamarock et al. 2008)
Domain	Single domain, 1120 × 1072 × 31 levels
Horizontal grid spacing	2 km
Duration	42 h, 0000 UTC 18 Aug–1800 UTC 19 Aug 2007
Initial and boundary conditions	6-hourly 1° GFS operational analyses
Convective parameterization	Explicit convection
Microphysical parameterization	Purdue–Lin (Chen and Sun 2002)
Boundary layer parameterization	YSU (Hong et al. 2006)
Surface layer parameterization	MM5 similarity (Skamarock et al. 2008)
Land surface parameterization	Unified Noah land surface model (Chen and Dudhia 2001)
Longwave radiation parameterization	RRTM scheme (Mlawer et al. 1997)
Shortwave radiation parameterization	Dudhia scheme (Dudhia 1989)

what would become TC Erin's lower-tropospheric inflow region during the reintensification period (not shown). This suggests that a third land surface feedback signal may also influence the reintensification process. This feedback, hereafter referred to as the "early rain" signal, is hypothesized to positively influence the boundary layer moisture content of such inflowing parcels via the same aforementioned land surface feedback processes, in turn potentially influencing deep moist convection and cyclone intensity. Support for such a hypothesis is given in part by the external moisture source contribution described by Emanuel et al. (2008).

The aim of this work is to determine the roles of the three aforementioned soil moisture content-related land surface feedback mechanisms to the reintensification of TC Erin. Specifically, utilizing a collection of convection-permitting, land surface feedback mechanism-varying real data model simulations of the reintensification period, we aim to quantify the effects of land surface feedbacks associated with the seasonal, early rain, and TC rainfall signals upon the intensity of the vortex. Such a study allows for the analysis of three key components to the reintensification process: understanding the total effects of soil moisture upon the thermodynamic environment (e.g., Trier et al. 2004; Santanello et al. 2005) associated with the reintensification, determining whether anomalously high soil moisture content is necessary for the observed reintensification to occur, and elucidation of other possible requisite factors to the reintensification process.

The remainder of this manuscript is structured as follows. Section 2 details the methodology behind the study, including mesoscale model simulation configuration and analysis methods. Section 3 describes the control simulation results with particular focus given to model verification and an analysis of TC-like vortex structure and environmental conditions. Section 4 describes the results from the remaining simulations, focusing upon the physical manifestation of the land surface feedbacks upon the reintensifying vortex. A discussion of the results and concluding remarks are presented in section 5.

2. Methodology

a. Control simulation

The control simulation in this work utilizes the Advanced Research Weather Research and Forecasting (WRF-ARW) mesoscale model version 3.1 (Skamarock et al. 2008). The WRF-ARW is a fully compressible, nonhydrostatic numerical model. A single simulation domain spanning 1120 × 1072 horizontal grid points with a horizontal grid spacing of 2 km and 31 vertical levels is utilized (Fig. 2). The simulation is carried out between 0000 UTC 18 August 2007 and 1800 UTC 19 August 2007, or from approximately 24 h prior to the start of the reintensification process through the midst of the decay process. Initial and boundary conditions for the model are provided by 6-hourly 1° National Centers for Environmental Prediction (NCEP) Global Forecast System (GFS; Environmental Modeling Center 2003) operational analyses. The Yonsei University (YSU; Hong et al. 2006) boundary layer parameterization, the Purdue–Lin (Chen and Sun 2002) microphysical parameterization,

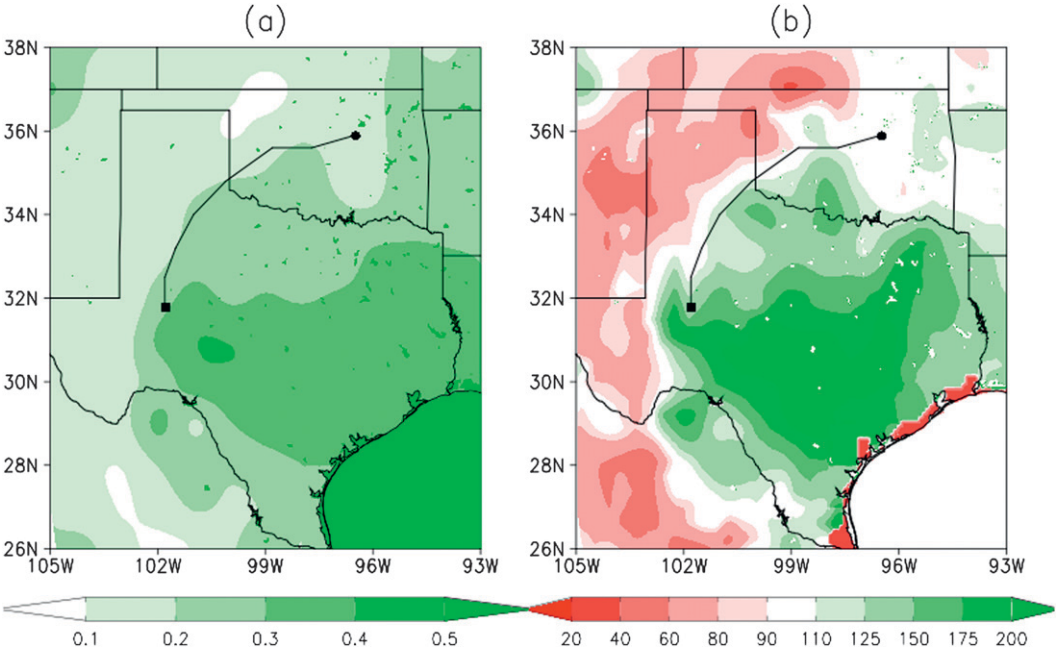

FIG. 3. (a) GFS-analyzed 18 Aug 2007 volumetric fractional 0–10-cm soil moisture content (units: dimensionless) across the southern Great Plains. The observed track of TC Erin (2007) is depicted by the solid black line. (b) 0–10-cm soil moisture percentage of climatology (units: dimensionless) for the 18 Aug 2007 GFS-analyzed soil conditions vs the August 1979–2006 NARR climatological mean. Green (red) values denote regions where soil moisture content was greater (lesser) in August 2007 than in the climatological mean. The observed track of the cyclone is depicted by the solid black line in both (a) and (b).

unified Noah (Chen and Dudhia 2001) land surface model parameterization, and the fifth-generation Pennsylvania State University–National Center for Atmospheric Research Mesoscale Model (MM5) similarity surface layer parameterization (as described by Skamarock et al. 2008) are utilized within this simulation. Convective processes are handled explicitly within the model. This configuration is similar, though not identical, to those used for studies of tropical cyclones over water (e.g., Davis et al. 2008) and severe convective systems over land (e.g., Weisman et al. 2008). A full list of model configuration parameters may be found in Table 1.

Soil moisture content within the control simulation is initialized from the soil moisture fields contained within the 0000 UTC 18 August 2007 1° NCEP GFS operational analysis. This dataset is chosen in part because of our desire to quantify and understand mesoscale, rather than microscale (e.g., updraft scale), impacts of soil moisture upon vortex evolution. Use of a higher-resolution product, such as that from the North American Mesoscale (NAM) model analysis, may introduce undesired—and potentially unrealistic—convective-scale feedbacks to the simulated evolution (S. Trier 2010, personal communication). This soil moisture content analysis is created using the Noah land surface model integrated within the operational GFS model and is thus consistent with the choice of the Noah land surface model in our control simulation. As noted by Koster et al. (2009), soil moisture content within numerical land surface model implementations is specific to the land surface model and is not a directly measured quantity, thus making the aforementioned consistency crucial to obtaining an accurate representation of the effects of soil moisture on the surface layer of the atmosphere. GFS-analyzed soil moisture fields in August 2007 (Fig. 3a) reflect greater model-synthesized soil moisture values across the southern Great Plains, particularly across much of Texas and southern Oklahoma, with lesser values noted across the southern High Plains, northern Oklahoma, and southern Kansas. As compared to August 1979–2001 climatological mean soil moisture conditions from the North American Regional Reanalysis (NARR; Mesinger et al. 2006) dataset, soil moisture content along the observed track of the cyclone is at or slightly above the climatological mean value for August with significantly moister (drier) conditions found to the right (left) of the track (excluding inland lakes in both regions; Fig. 3b). As noted by Arndt et al. (2009), this positive soil moisture anomaly likely stems from an anomalously wet March–July 2007 across much of Oklahoma and Texas. Though weather

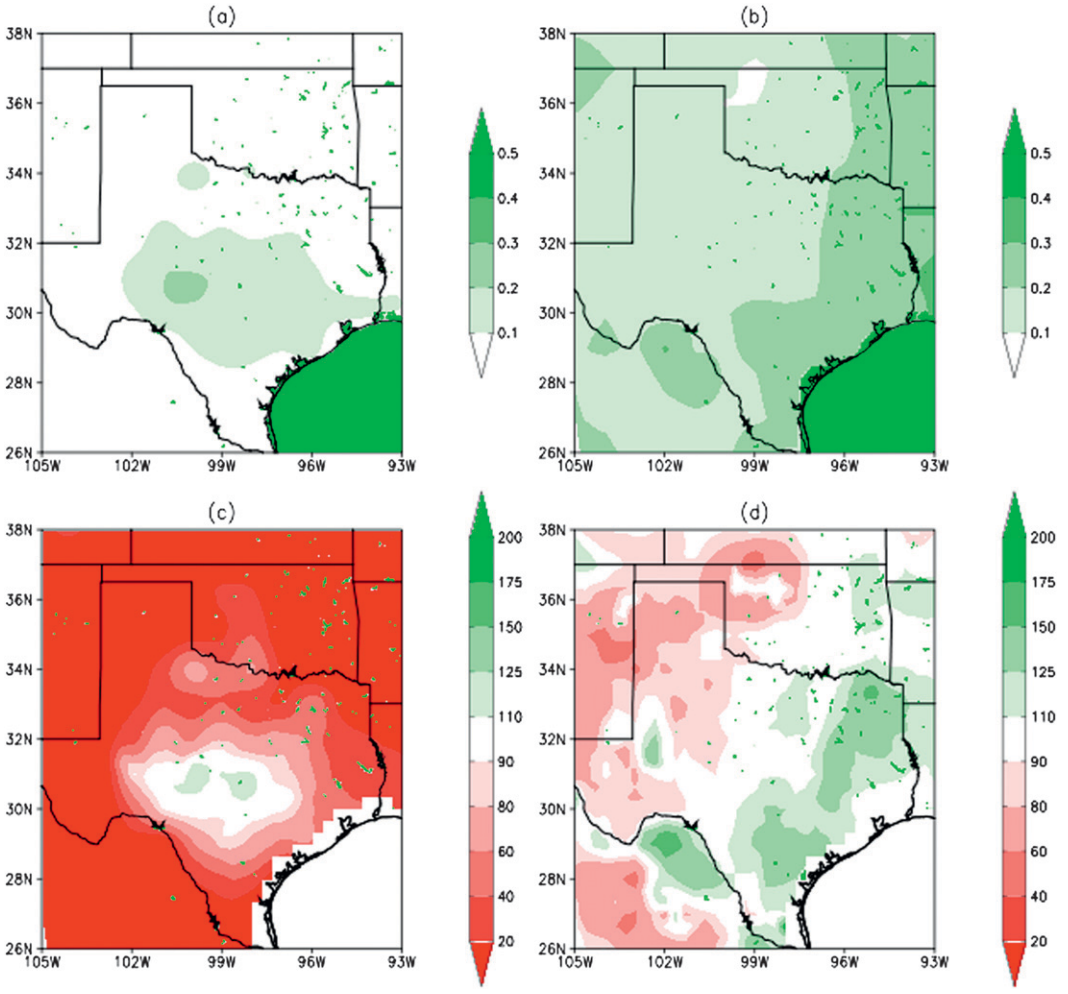

FIG. 4. (a) "Early Rain" simulation soil moisture input, or the GFS-analyzed 0000 UTC 18 Aug 2007 volumetric fractional 0–10-cm soil moisture content minus the GFS-analyzed 0000 UTC 15 Aug 2007 volumetric fractional 0–10-cm soil moisture content (units: nondimensional). (b) "Seasonal" simulation soil moisture input, or the GFS-analyzed 0000 UTC 15 Aug 2007 volumetric fractional 0–10-cm soil moisture content (units: nondimensional). (c) Percentage of climatology of the field in (a) from the August 1979–2006 NARR climatological mean. (d) As in (c), but for the field depicted in (b).

conditions in August 2007 preceding the reintensification of TC Erin were generally hot and dry, a substantial positive soil moisture anomaly remained across the southern Great Plains through the landfall of TC Erin on 16 August 2007 and was augmented on 16–17 August 2007 by substantial rainfall associated with TC Erin itself across central and southern Texas (Fig. 1).

b. Sensitivity simulation formulation

In addition to the control simulation noted above, eight additional simulations are performed. Each of these additional simulations utilizes the same configuration as the control simulation apart from the initial representation of soil moisture conditions within the model, whether rainfall is allowed to modify soil moisture content within the model, or both. Specifically, whereas the control simulation includes all three land surface feedback signals described in section 1, seven of the eight additional simulations contain only zero, one, or two of these signals. (The remaining simulation utilizes climatological soil moisture conditions and is conducted to compare the influences of each of the three aforementioned signals upon the reintensification process to that from climatology.) Studying the reintensification of TC Erin (2007) in this way allows for the quantification of each signal's impacts upon the intensity of the vortex both independently as well as in conjunction with one or more additional signals.

The soil moisture content input used to represent the seasonal signal is obtained from the 0000 UTC 15 August 2007, or before Erin's formation and subsequent landfall,

TABLE 2. Detail behind the formulation of each of the sensitivity simulations conducted in this study.

Simulation	Soil moisture initialization	Can rainfall modify soil moisture?
Null	Initially dry soils	No
TC Rain	Same as "Null"	Yes
Early Rain	0000 UTC 18 Aug 2007 1° GFS soil moisture initialization minus the 0000 UTC 15 Aug 2007 1° GFS soil moisture initialization (Figs. 4a,c).	No
Seasonal	0000 UTC 15 Aug 2007 1° GFS soil moisture initialization (Figs. 4b,d)	No
TC+Early	Same as "Early Rain"	Yes
TC+Seasonal	Same as "Seasonal"	Yes
Early+Seasonal	Same as control (Fig. 3).	No
Average Soil	Mean August 1979–2006 NARR-analyzed soil moisture content	Yes

GFS analysis (Figs. 4b,d). Soil moisture content is near normal across much of central Oklahoma and Texas and slightly below (above) normal across areas to the west (east). The soil moisture content input used to represent the early rainfall signal is obtained by subtracting the seasonal signal input soil moisture content from the control simulation soil moisture content input (Figs. 4a,c). Where such a value is below zero, a physically unrealistic situation, initial soil moisture content is set to zero. In this input, soil moisture content is slightly above that from climatology across central Texas, highlighting the significant contribution of TC Erin's early rains to the anomaly depicted in Fig. 2b. The TC rainfall signal is tested by modifying the Noah land surface model code to allow (or disallow) the modification of soil moisture content due to rainfall during the mesoscale model simulation. A completely dry soil moisture content input is used in the two simulations that independently test this TC rainfall signal. A full summary of these simulations may be found in Table 2.

3. Results: Control simulation

a. Model verification

The rarity of the observed reintensification necessitates a complete verification of the simulated reintensification process in order to correctly interpret insight obtained from the simulations. The simulated and observed track and intensity are depicted in Fig. 5. The control simulation generally exhibits a slow along-track and eastward cross-track bias (Fig. 5a). Position errors are on the order of 100–150 km throughout much of the simulation (not shown). The majority of these errors arise as a result of an unrealistic southward displacement of the initial vortex within the GFS-based model initialization and the spinup of the vortex within the first 6 h of the simulation. With respect to intensity (Fig. 5b), good agreement between the simulation and the NHC best-track intensity analysis is noted throughout the first 21 h of the control simulation. The control simulation is able to reasonably reintensify the cyclone early on 19 August, though it is offset by approximately 2 h from the NHC best-track analysis, and it decays it at a similar rate to that observed later on 19 August. Given similar soil characteristics across northern Texas to those over western Oklahoma (not shown), it is not believed that

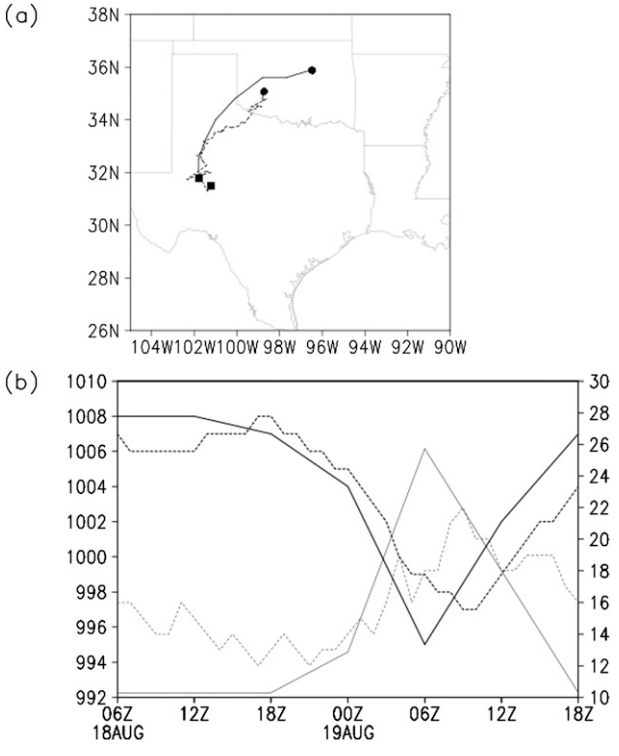

FIG. 5. (a) Control simulation (dashed) and NHC best-track (solid) tracks of TC Erin (2007) between 0000 UTC 18 Aug 2007 (location denoted by a filled square) and 1800 UTC 19 Aug 2007 (location denoted by a filled circle). (b) Control simulation (dashed) and NHC best-track (solid) minimum sea level pressure (hPa; thick lines; left axis) and maximum instantaneous 10-m wind magnitude (m s^{-1}; thin lines; right axis) between 0600 UTC 18 Aug 2007 and 1800 UTC 19 Aug 2007.

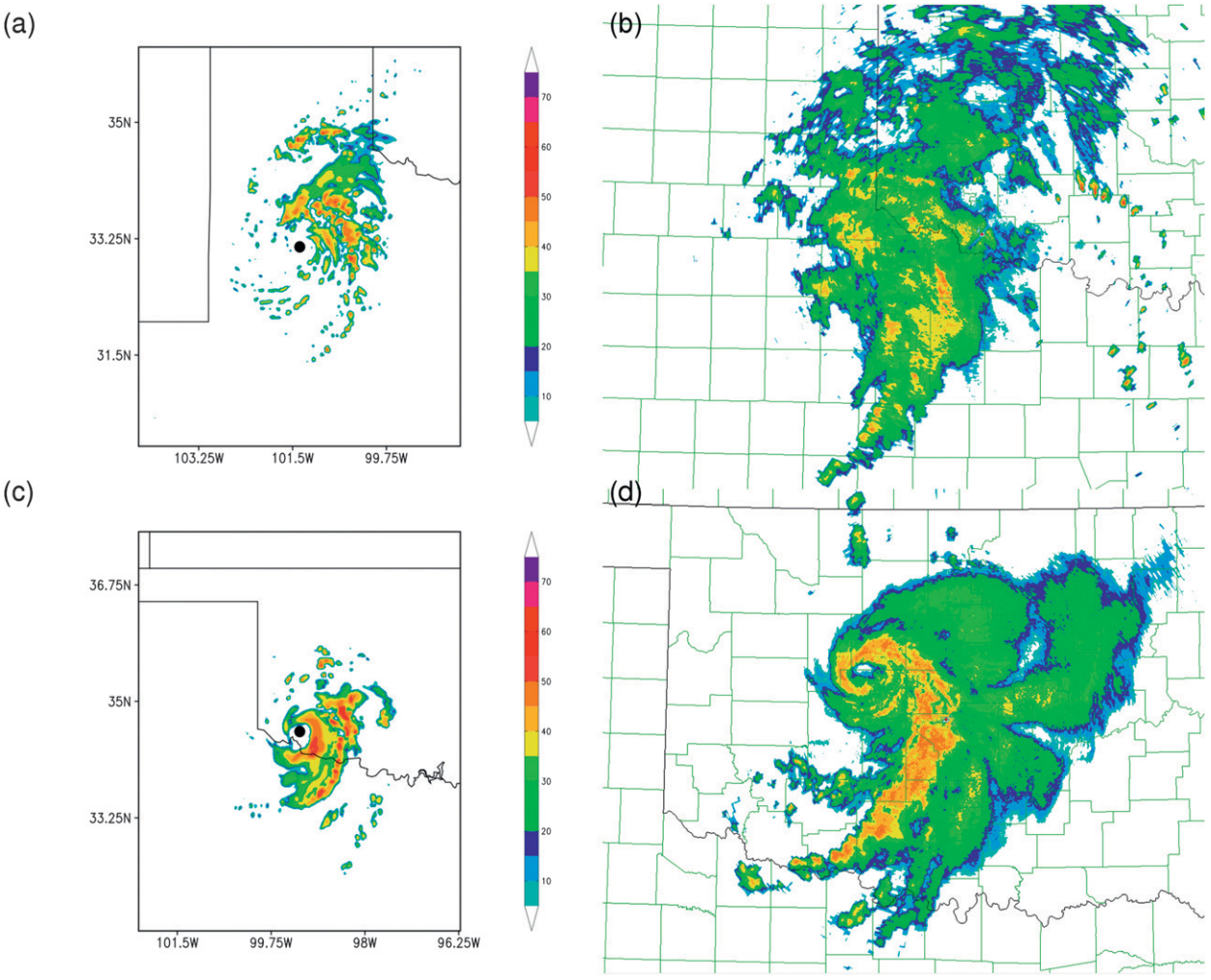

FIG. 6. (a) Control simulation composite reflectivity (dBZ) product valid at 1800 UTC 18 Aug 2007. The center of the simulated vortex is denoted by the filled circle. (b) Lubbock, TX, WSR-88D level-II 0.5° tilt base reflectivity (dBZ) valid at 1800 UTC 18 Aug 2007. (c) As in (a), but valid at 1000 UTC 19 Aug 2007. (d) As in (b), but from the Oklahoma City, OK, WSR-88D radar and valid at 1000 UTC 19 Aug 2007. The color scale for (b),(d) is as in (a),(c).

the errors in the simulated track substantially influence the results presented in this work from the standpoint of land surface characteristics.

During the daytime hours on 18 August, the simulated vortex maintains its intensity (Fig. 5b) while convection in its proximity is focused along outer rainbandlike features (Fig. 6a). This is in line with available radar observations (Fig. 6b) despite the inability of the control simulation to fully capture the stratiform rain region in the midst of the isolated convection. This is believed to be due to limitations in the Purdue–Lin microphysical parameterization employed within this study (Done et al. 2004). This also agrees with the typical daytime structure of precipitation and convection associated with mesoscale convective vortices (MCVs) over land (e.g., Trier et al. 2000). During the reintensification process, the simulated vortex becomes better defined with a partial eyelike feature observed at its peak intensity near 1000 UTC 19 August (Fig. 6c). This simulated reflectivity structure is in good agreement with available radar observations (Fig. 6d) despite the simulated location error.

Next, a quantification of the simulated mesoscale environment and how it compares to available operational analysis-synthesized observations early in the reintensification process is presented. At the outset of the reintensification period, the vortex is embedded within a moist, modestly unstable thermodynamic environment (Figs. 7a,b). Approximately 1000–1500 J kg^{-1} surface-based convective available potential energy (CAPE) is found ahead and to the right of the simulated vortex's track along a near-surface convergence axis extending southwestward from near 32.25°N, 100°W toward 30°N,

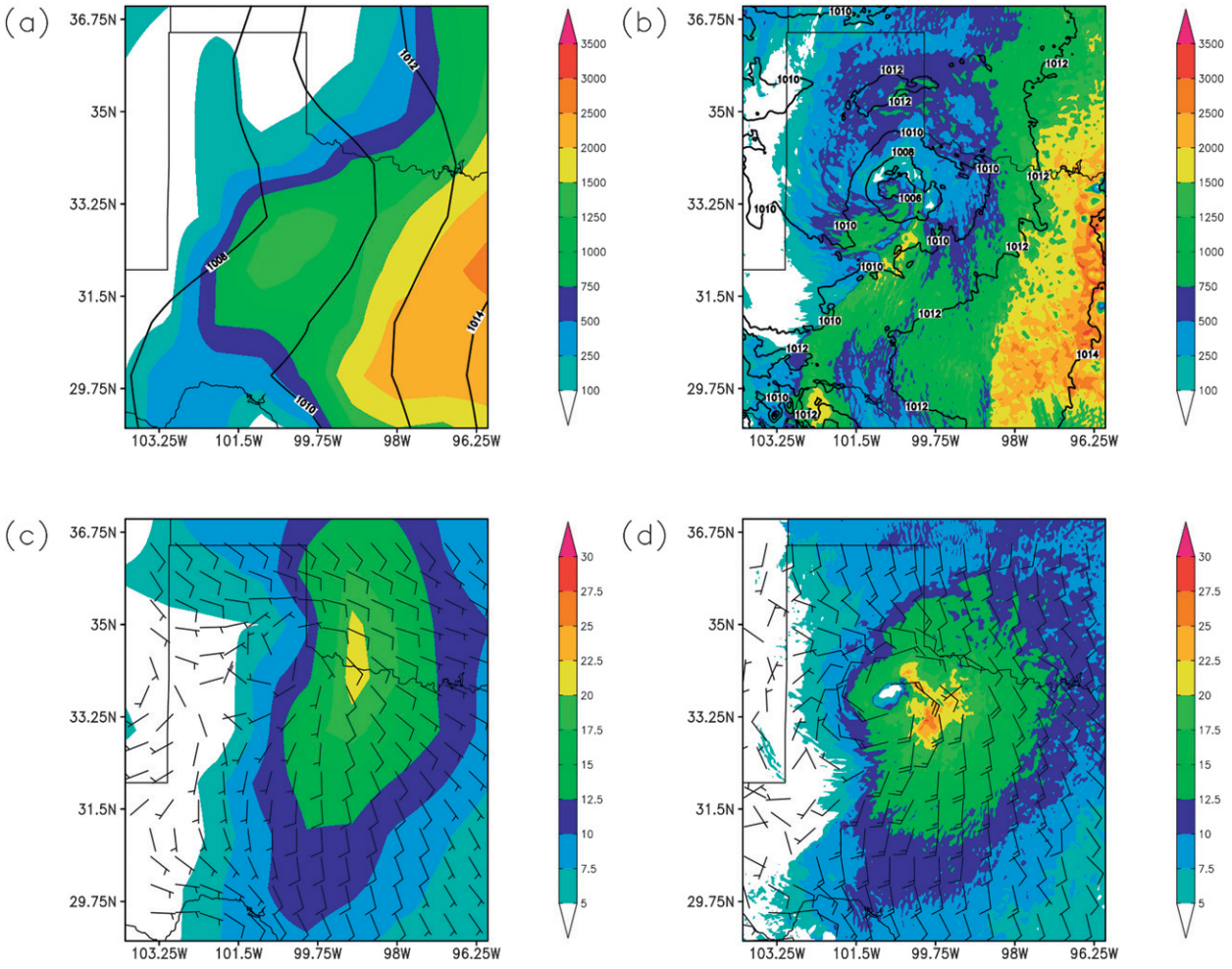

FIG. 7. (a) Minimum sea level pressure (hPa; contoured) and surface-based convective available potential energy (J kg^{-1}; shaded) from the GFS analysis valid at 0000 UTC 19 Aug 2007, or 24 h into the control simulation. (b) As in (a), but from the control simulation. (c) As in (a), but for 850-hPa wind speed (m s^{-1}; shaded) and 10-m winds (kt, barbs; 1 kt = 0.5144 m s^{-1}). (d) As in (c), but from the control simulation.

102.5°W (Figs. 7b,d). These fields are in good agreement with available observations as synthesized by the 0000 UTC 19 August 2007 GFS analysis (Figs. 7a,c) and to a 0000 UTC upper-air sounding from Dallas–Ft. Worth, Texas (Fig. 8a). Of particular note in both the control simulation (Fig. 8b) and available observations (Fig. 8a) is a deeply moist—though not moist neutral—sounding profile. As will be shown later, the simulated (and presumably observed) departures from moist neutrality do not appear to significantly hinder the reintensification process via the development of surface cold pools and accompanying near-surface divergent wind profiles that would hinder near-surface vertical vorticity growth [e.g., as described by Fritsch et al. (1994) and others].

Dynamically, a well-defined 850-hPa lower-tropospheric jet (LLJ) in excess of 20 m s^{-1} aligned with the previously discussed near-surface convergence and instability axes is observed immediately east of the vortex in both the control simulation and available observations (Figs. 7c,d). The LLJ aids in focusing boundary layer lift and convergence immediately ahead of the remnant vortex (e.g., Schumacher and Johnson 2009). Furthermore, the vertical structure of the lower-tropospheric wind profile along the LLJ exhibits veering of the winds with increasing height (Fig. 8), indicative of warm advection into the environment of the remnant vortex that aids in maintaining the thermodynamic profile against adiabatic, evaporative, and radiational cooling processes. The mid-to-upper-tropospheric pattern in the immediate vicinity of the vortex is dominated by the weak midtropospheric reflection of the remnant vortex in both the control simulation (not shown) and in reality (Monteverdi and Edwards 2010, their Fig. 11). The weak (compared to the boundary layer) reflection of the vortex in the midtroposphere is indicative of a warm-core (or TC like) structure to the vortex.

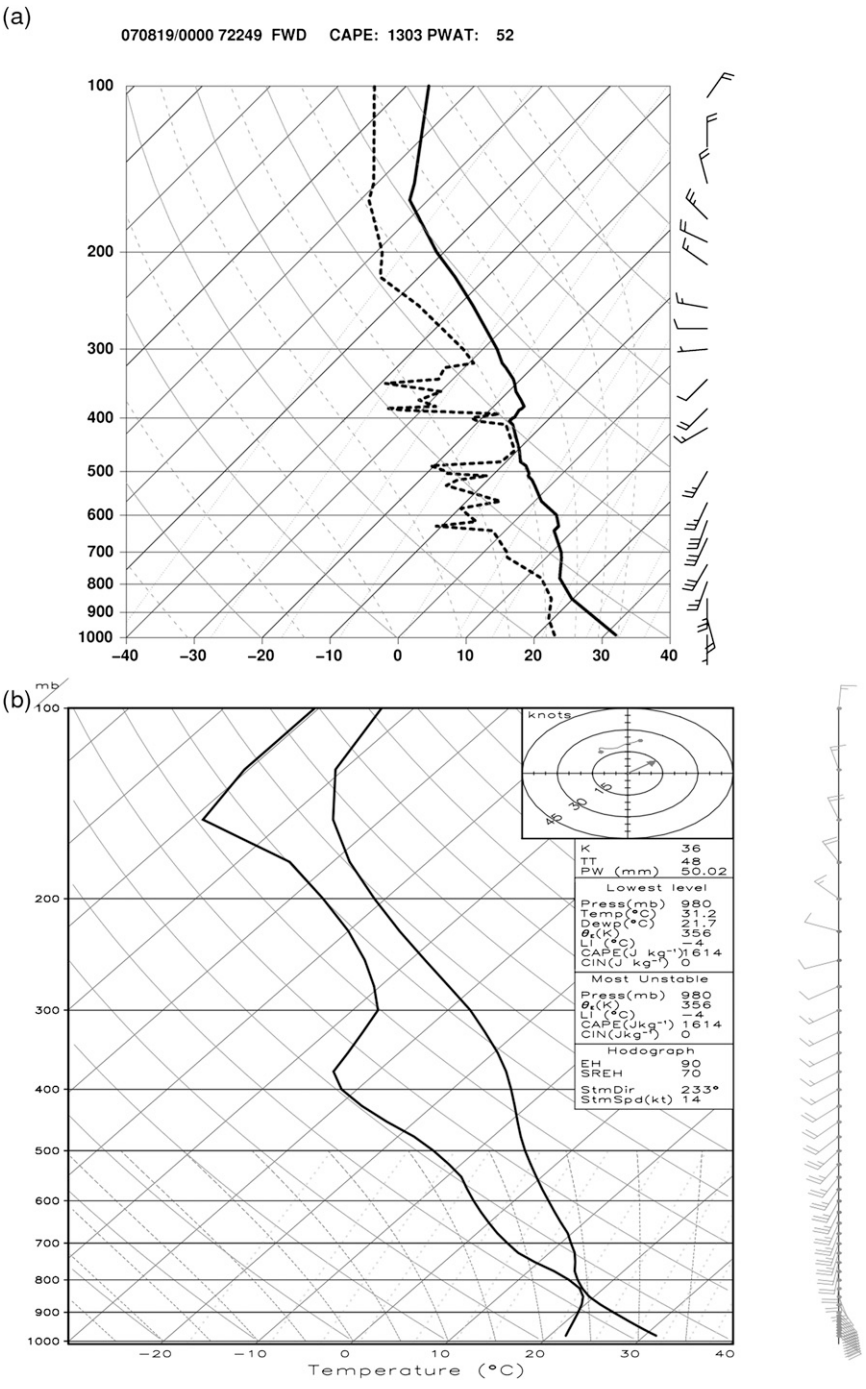

FIG. 8. (a) Observed Dallas–Ft. Worth, TX, sounding valid at 0000 UTC 19 Aug 2007. (b) Dallas–Ft. Worth, TX, sounding valid at 0000 UTC 19 Aug 2007 as obtained from the control simulation.

As a result of the verification presented above, the control simulation is believed to be a sufficiently accurate depiction of the evolution of the remnant TC and its environment before, during, and after the reintensification period on 19 August 2007. Despite the caveat that the evolution of the simulated vortex may not be equivalent to reality, these findings breed confidence that the numerical model can provide reasonable insight into the physical processes associated with the observed reintensification process.

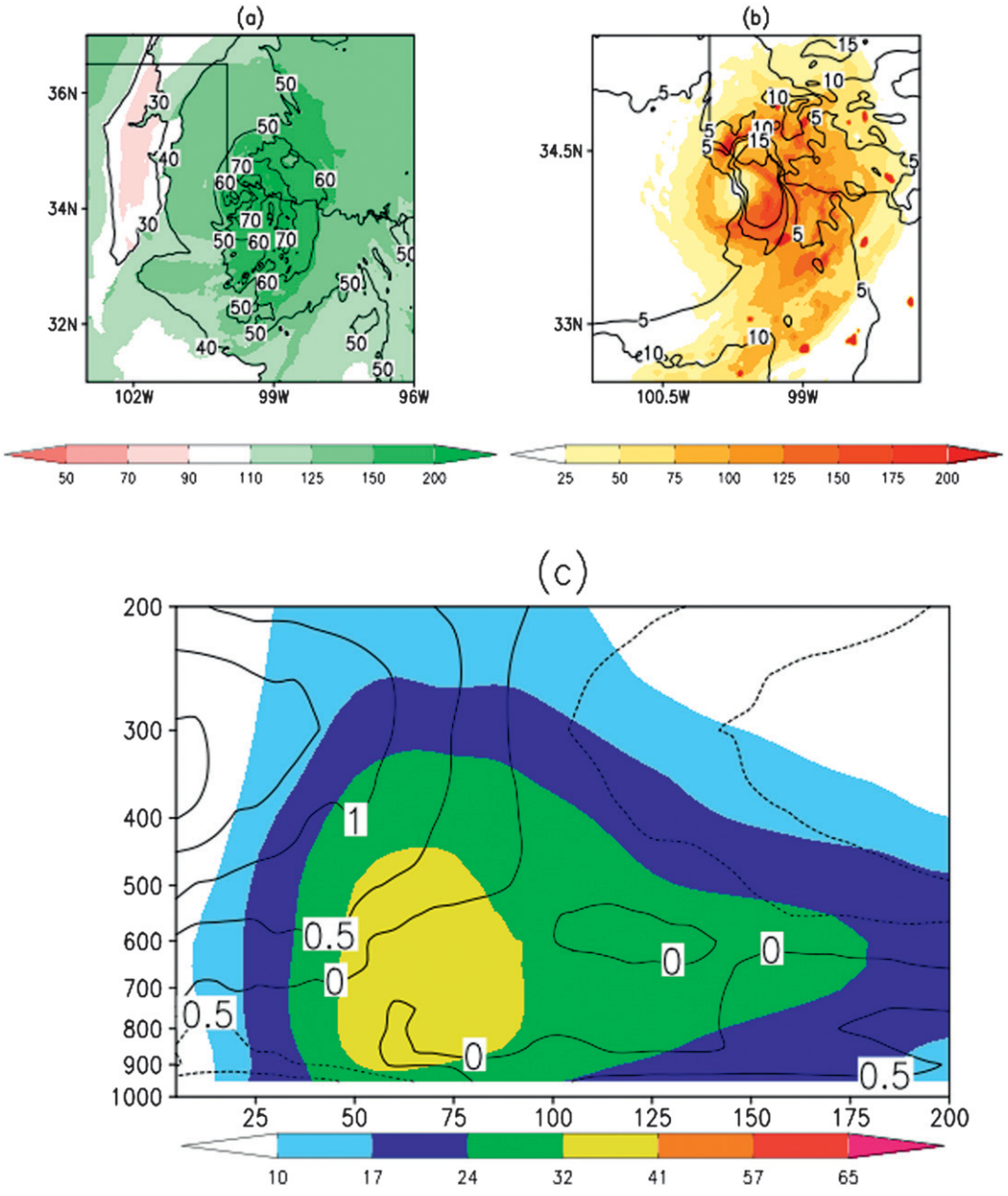

FIG. 9. (a) Model-simulated total precipitable water (contoured; units: mm) valid at 0600 UTC 19 Aug 2007 and percentage departure of the total precipitable water from the August 1979–2001 NARR climatological precipitable water (shaded). (b) Model-simulated surface latent heat flux (shaded; units: W m^{-2}) and 850–300-hPa vertical wind shear with the azimuthally averaged tangential wind of the vortex removed (contoured; units: m s^{-1}) valid at 0600 UTC 19 Aug 2007. (c) Vertical profile of the azimuthally averaged tangential wind (shaded; kt) and potential temperature anomaly from the radial mean (contoured; K) between the 5–200-km radius (lower axis) from the center of the simulated vortex valid at 0600 UTC 19 Aug 2007.

b. Examination of TC-like vortex structure and environmental conditions

Whether TC Erin (2007) reintensified as a tropical cyclone or not has been the subject of much debate in the literature (e.g., Brennan et al. 2009; Monteverdi and Edwards 2010). While the primary focus of this paper is upon land surface influences upon the reintensification process, it is nevertheless worthwhile to examine the simulated environment within which TC Erin (2007) reintensified and the simulated vortex structure that results from the reintensification process.

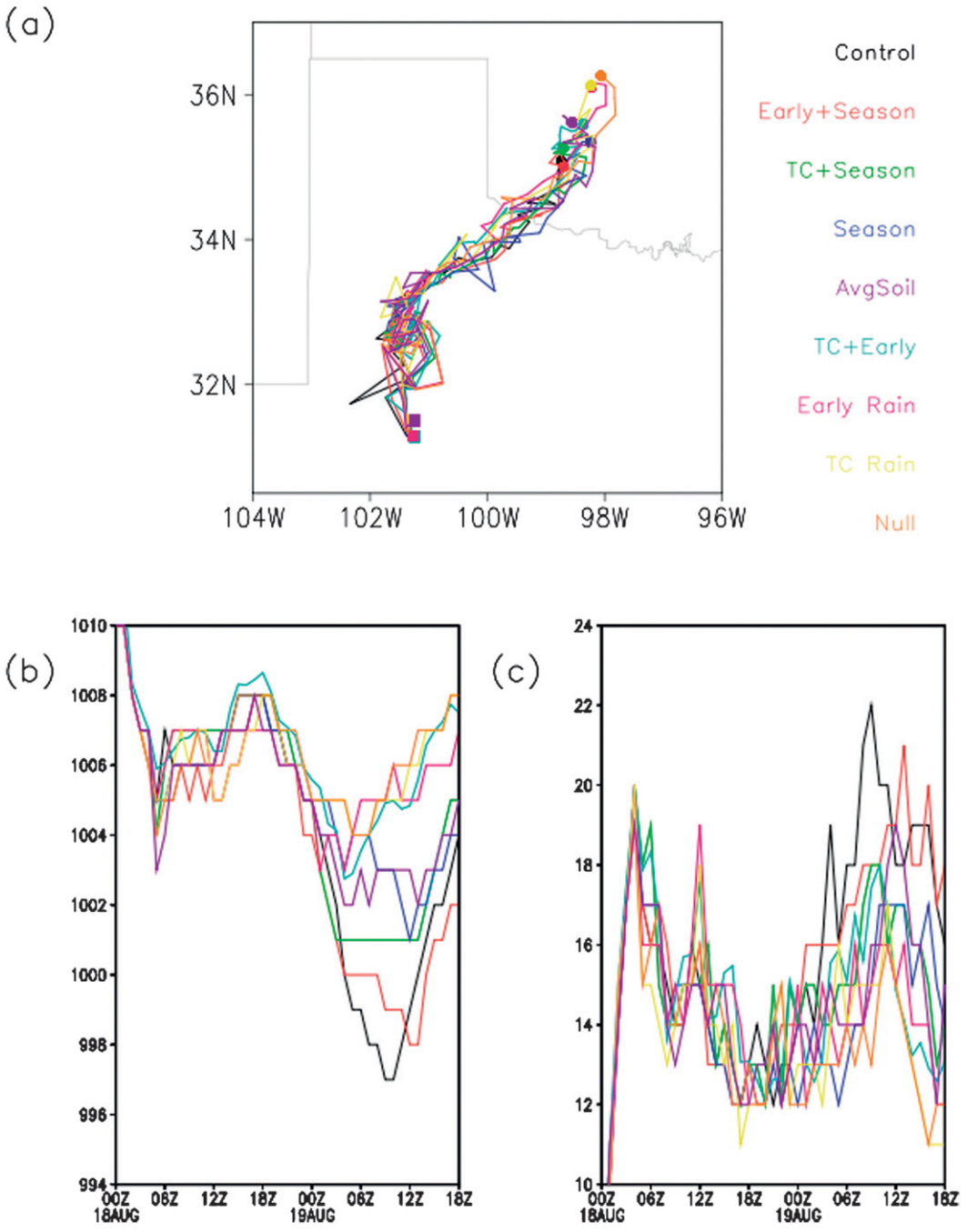

FIG. 10. (a) Simulated tracks from each of the eight simulations conducted in this study. The squares (circles) denote the vortex location at the start (end) of the simulation. (b) Simulated vortex mean sea level pressure trace (hPa) from each of the eight simulations conducted in this study. (c) Simulated vortex maximum sustained 10-m wind speed trace ($m\ s^{-1}$) from each of the eight simulations conducted in this study. The color legend for each is depicted in the upper-right portion of the diagram.

Gray (1968) and other subsequent works highlighted several key environmental factors important for TC formation and development. Specifically, these include the following: 1) a weakly nonzero Coriolis parameter, 2) weak vertical wind shear, 3) prolonged lower-tropospheric convergence, 4) a preexisting disturbance, 5) a deep moist troposphere, and 6) sufficiently warm sea surface temperatures (>26.5°C). Conditions 1, 3, and 4 are met by the presence of the remnant TC Erin (2007) across Texas at latitudes greater than 30°N. An examination

TABLE 3. Summary of the minimum sea level pressure (hPa), peak 10-m wind magnitude (m s^{-1}), and peak 700-hPa circulation inside of 75-km radius ($\times 10^6$ m^2 s^{-1}) in the vicinity of the simulated vortex from each of the simulations described in Table 2.

Simulation name	Minimum sea level pressure (hPa)	Peak 10-m wind speed (m s^{-1})	Peak 700-hPa circulation inside 75 km radius ($\times 10^6$ m^2 s^{-1})
Control	997 hPa	22 m s^{-1}	8.30
Early+Seasonal	998 hPa	21 m s^{-1}	8.03
TC+Seasonal	1001 hPa	18 m s^{-1}	6.59
Seasonal	1001 hPa	17 m s^{-1}	7.22
Average Soil	1002 hPa	19 m s^{-1}	6.73
TC+Early	1002 hPa	18 m s^{-1}	7.06
Early Rain	1003 hPa	16 m s^{-1}	6.44
TC Rain	1004 hPa	16 m s^{-1}	6.35
Null	1004 hPa	16 m s^{-1}	6.12

of the moisture fields in the environment of the remnant vortex during the reintensification period suggests that condition 5 is met as well, with total precipitable water values in excess of 50–60 mm over a large region near and ahead of the vortex (Fig. 9a). This deeply moist environment was established over the southern Great Plains via deep layer moisture transport east of TC Erin (2007) from the Gulf of Mexico (e.g., Schumacher et al. 2011, their Fig. 3). As noted by Arndt et al. (2009) and depicted in Fig. 9a, such moisture content is highly abnormal for August across the southern Great Plains. A concordant examination of the 850–300-hPa vertical wind shear with the azimuthally averaged tangential wind of the vortex removed suggests that vertical wind shear was light to moderate at approximately 5–10 m s^{-1} in the environment of the vortex (Fig. 9b). The area of enhanced vertical wind shear immediately east of the vortex is a reflection of the asymmetric nature of the vortex (with stronger tangential winds east and weaker tangential winds west of the vortex center) and aforementioned lower-tropospheric jet into which the cyclone passed during the reintensification period. Such an environment has previously been characterized as favorable for warm-core MCV vortex intensification and longevity via the promotion of an upright vortex core (e.g., Menard and Fritsch 1989; Fritsch et al. 1994; Yu et al. 1999; Trier et al. 2000; Davis and Trier 2007).

Thus, of the parameters set forth by Gray (1968), only condition 6, the sea surface temperature criterion, is not met. However, Emanuel et al. (2008) noted that surface latent heat fluxes of 150–200 W m^{-2} observed with reintensifying TCs over Australia can support near-hurricane intensity from the TC-like disturbances over

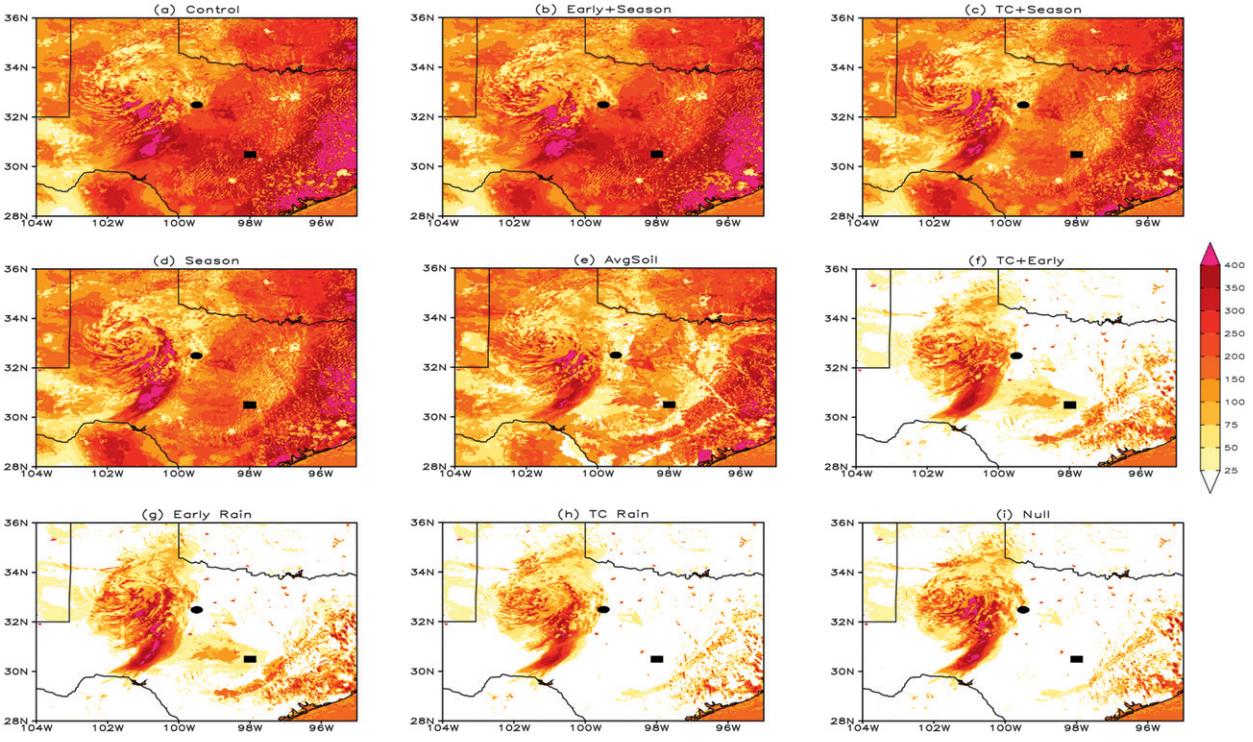

FIG. 11. Surface latent heat flux magnitude (W m^{-2}) valid at 1800 UTC 18 Aug 2007 from the (a) Control, (b) Early+Seasonal, (c) TC+Seasonal, (d) Seasonal, (e) Average Soil, (f) TC+Early, (g) Early Rain, (h) TC Rain, and (i) Null simulations. Values are shaded according to the color bar in (f). Circles (squares) depict the location of the soundings in Fig. 12 (Fig. 13).

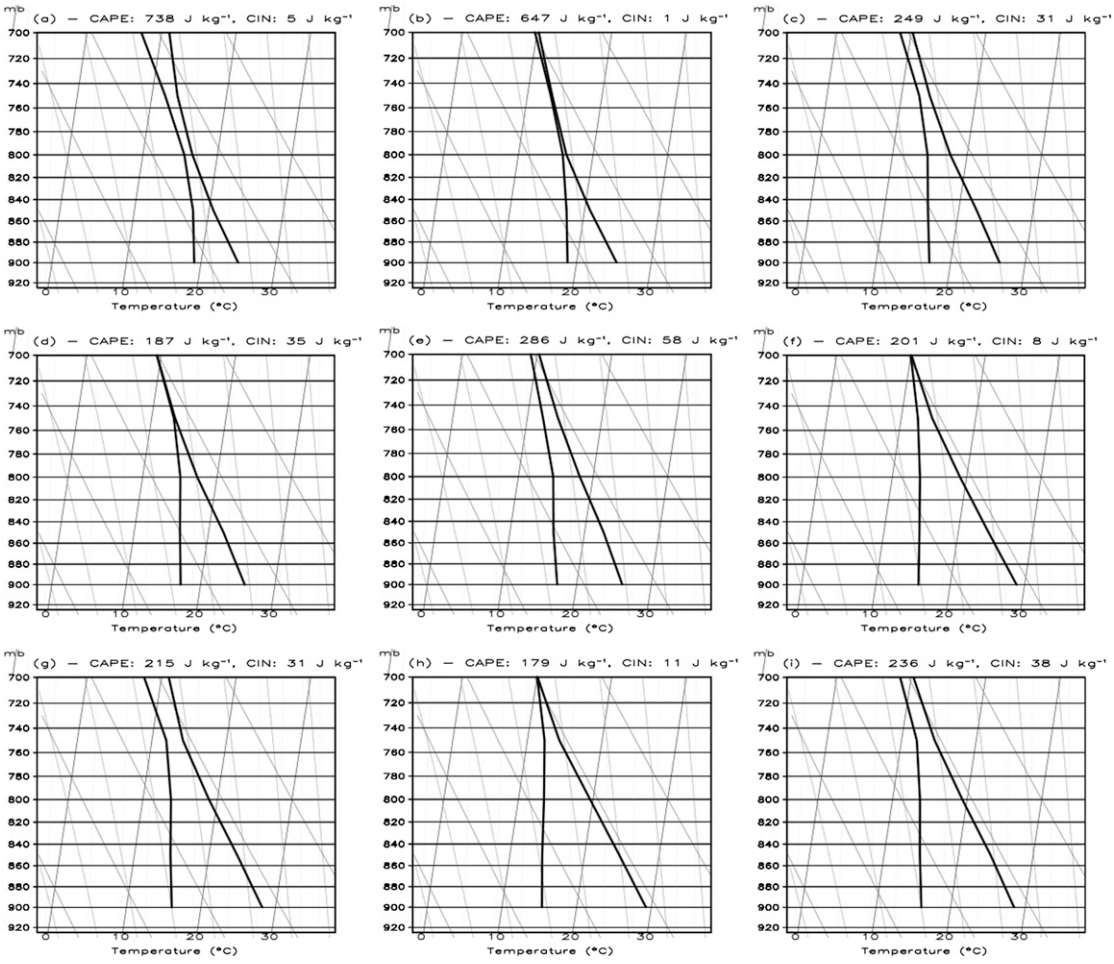

FIG. 12. Skew T–log$p$ diagrams between 925–700 hPa valid at 0000 UTC 19 Aug 2007 at 32.5°N, 99.5°W, or immediately east of the simulated vortex, from the (a) Control, (b) Early+Seasonal, (c) TC+Seasonal, (d) Seasonal, (e) Average Soil, (f) TC+Early, (g) Early Rain, (h) TC Rain, and (i) Null simulations. Total surface-based convective available potential energy and convective inhibition are listed at the top in (a)–(i).

land. Similarly, Montgomery et al. (2009) presented evidence suggesting that so-called trade wind values of surface latent heat fluxes—approximately 150 W m^{-2}—can support the development of TCs. In Fig. 9b, the surface latent heat fluxes associated with the simulated reintensification of TC Erin (2007) are presented. Widespread surface latent heat fluxes in excess of 100 W m^{-2} are noted near and ahead of the simulated vortex with localized areas of surface latent heat fluxes in excess of 150 W m^{-2} noted near the vortex itself. A complete examination of the energetics behind the reintensification of TC Erin (2007) is beyond the scope of this work. Nevertheless, coupled with the favorable environmental conditions noted above, the presence of surface latent heat flux values supportive of TC development in its environment suggests that TC Erin (2007) at least had the *ability* to reintensify as a TC while over Oklahoma.

An examination of the simulated structure of the vortex near its peak intensity suggests that TC Erin (2007) had a TC-like structure during the reintensification phase (Fig. 9c). The maximum azimuthally averaged tangential winds associated with the vortex are of minimal tropical storm intensity and are found near the top of the boundary layer between 50–75-km radius from the center of the cyclone. The azimuthally averaged tangential wind decays with increasing altitude, implying a deep warm-core structure to the vortex. Radially inward of this wind maximum, a warm potential temperature anomaly of in excess of 2 K is found in the upper troposphere. The intensity and altitude of this anomaly is similar to that observed with mature TCs of modest intensity. In the aggregate, the simulated vortex appears to exhibit a TC-like structure, in line with the findings of Monteverdi and Edwards (2010).

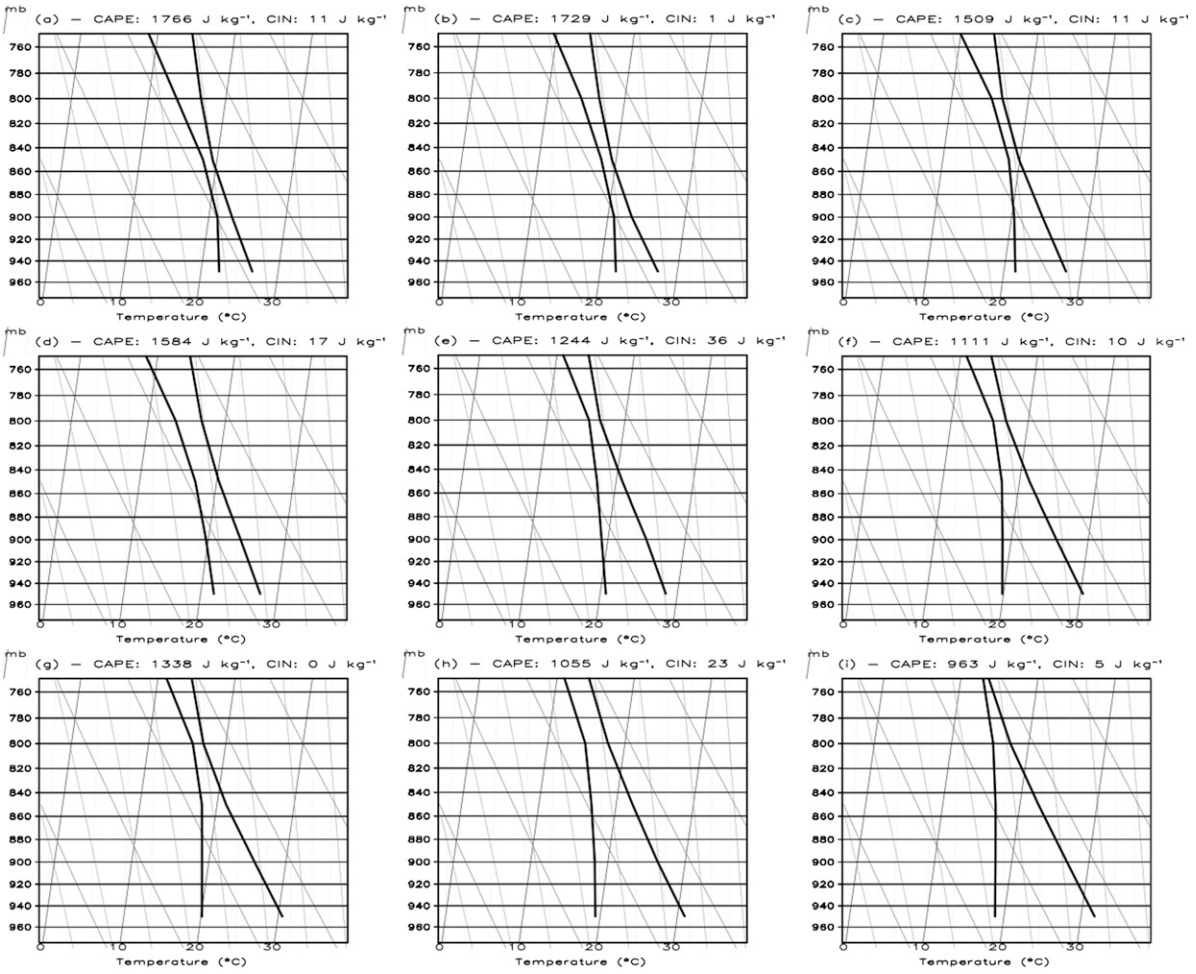

FIG. 13. As in Fig. 12, but at 30.5°N, 98.0°W, or within the outer inflow region of the simulated vortex, and between 975–750 hPa.

It should be noted that, operationally, Erin was not considered to be a TC while over Oklahoma because of the relatively short longevity of the deep moist convection associated with the vortex (Brennan et al. 2009). Specifically, Brennan et al. (2009) claim that upper-tropospheric forcing appeared to be a dominant mechanism in the convective development process, though no evidence is presented to that effect. Though the subject of convective development and organization with Erin is the subject of ongoing research (see section 5 for more), we note that transient upper-tropospheric forcing has been shown to positively influence the intensity of classified TCs over both water (e.g., Hanley et al. 2001) and land (Bosart and Lackmann 1995; Bassill and Morgan 2006). While it is true that the deepest, most intense convection associated with Erin while over land had a short longevity over Oklahoma, an analysis of radar and satellite imagery during 17–19 August 2007 shows that Erin was not completely devoid of organized moist convection throughout this time (not shown). Thus, in light of these considerations and the evidence presented above, we feel that Erin was effectively a TC while over Oklahoma. Implications of this are discussed in section 5.

4. Results: Sensitivity simulations

a. Basic simulation results

The intensity changes within each of the simulations conducted in this study are depicted in Figs. 10b,c and Table 3. Track differences between each simulation are minimal (Fig. 10a), suggesting that the differences seen between simulations are due to the influence of the varying soil conditions rather than substantial track—and thus not-soil condition-related environmental—differences. Substantial along-track deviations between simulations occur only when the automated vortex tracker (based upon the location of the maximum 700-hPa circulation magnitude within a 75 $\times$ 75 km^2 box) identifies the center of the

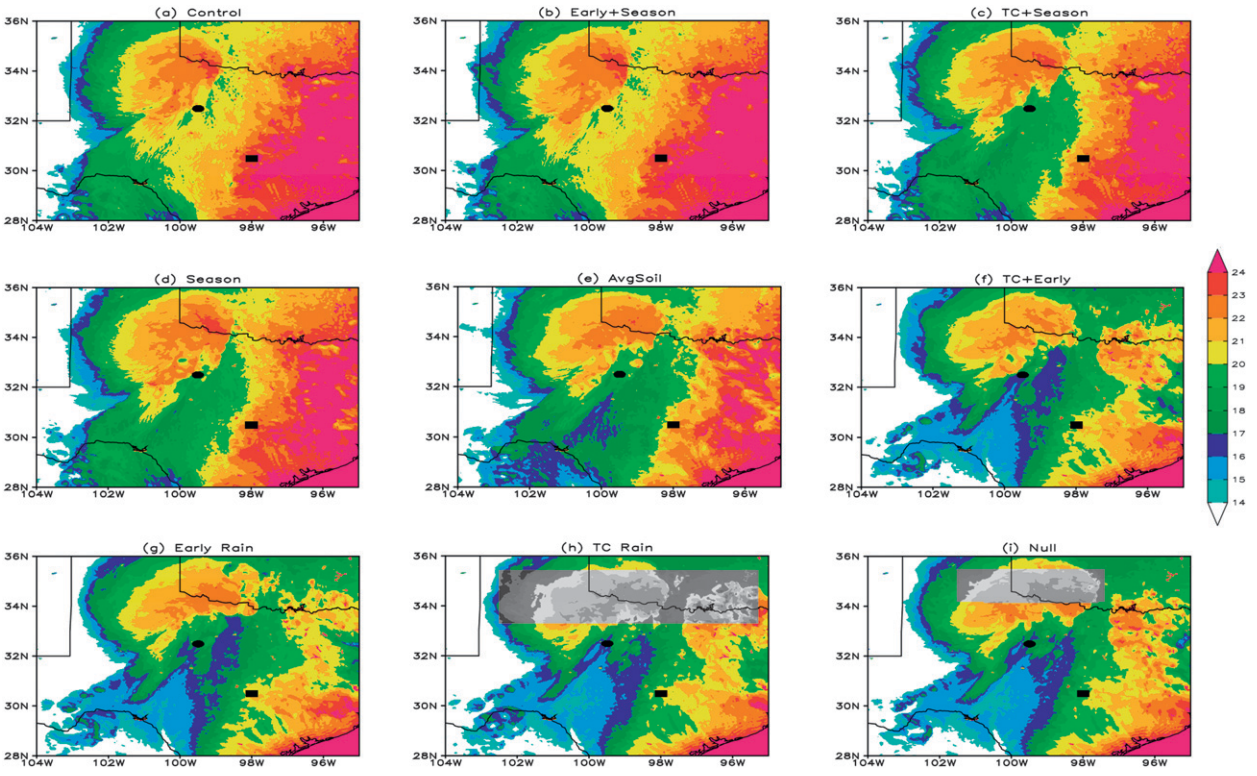

FIG. 14. As in Fig. 11, but for 2-m dewpoint (°C) and valid at 0000 UTC 19 Aug 2007.

vortex with a transient meso-γ-scale circulation maximum rather than the primary meso-α-scale circulation. In each simulation, the simulated vortex begins to deepen during the late afternoon hours on 18 August 2007, similar to reality, and reaches a peak intensity within 3 h on either side of 0600 UTC 19 August 2007. Minimum sea level pressures range from 997 to 1004 hPa and maximum sustained 10-m wind speeds range from 16–22 m s^{-1}. The most intense simulated vortex is approximately 35% stronger than the weakest simulated vortex in terms of peak 700-hPa circulation magnitude (Table 3). Despite the variance in soil moisture conditions, the vortex in each simulation is able to deepen by at least 4 hPa early on 19 August 2007. Note, however, that the simulated vortex is also able to deepen by 2 hPa in this same time period in a simulation identical to the "Null" simulation except in which all surface latent heat fluxes are turned off (not shown). This suggests that while much of the simulated reintensification may be significantly influenced by the underlying soil moisture content, a small portion may be due to other processes (e.g., plant transpiration and other factors discussed in section 5).

Three key findings arise from the results presented in Fig. 10 and Table 3. First, soil moisture content across the domain appears to be related to the intensity of the reintensifying vortex. Simulations which featured wetter, more waterlike soil conditions (e.g., Control and Early+Seasonal) permitted the greatest deepening of the simulated vortex. Conversely, simulations which featured drier, more droughtlike soil conditions (e.g., TC Rain and Null) permitted the weakest deepening of the simulated vortex. This is similar to the previously demonstrated response of TC-like vortices to increasingly waterlike land surface in the works of Shen et al. (2002) and Tuleya (1994). The physics of how soil moisture content influences boundary layer structure in the environment of the simulated vortex and, in turn, the intensity of the simulated vortex, are discussed in the following section.

Second, of the three signals tested, the seasonal rainfall signal (e.g., Figs. 4b,d) appears to contribute most favorably to the final intensity of the vortex when considered in isolation. To first order, this is in line with the Emanuel (2008) hypothesis, though the inability of the seasonal simulation to fully replicate the peak observed intensity of the vortex suggests that it alone can, at best, explain only a portion of the land surface impacts upon TC Erin's reintensification. It should be noted, however, that its impact over that resulting from climatological soil moisture conditions (cf. Seasonal to Average Soil in Table 3) is minor and likely statistically insignificant in nature. This suggests

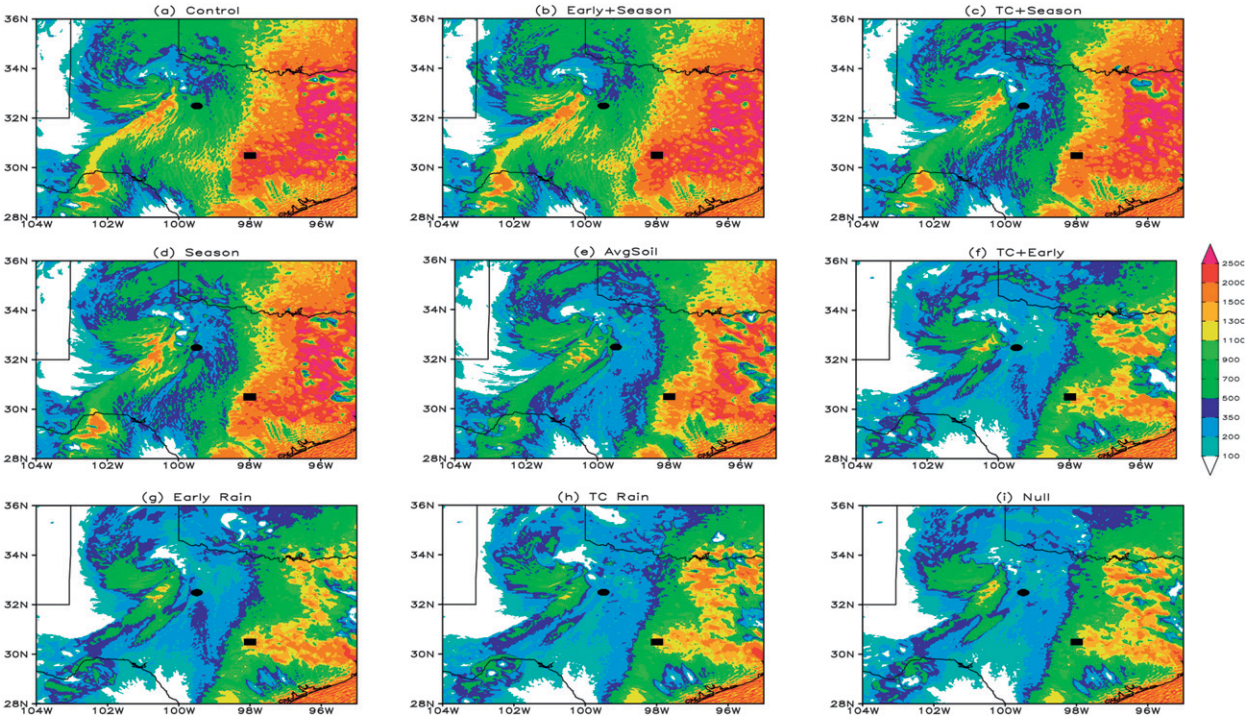

FIG. 15. As in Fig. 14, but for surface-based convective available potential energy (J kg^{-1}).

that the abnormally moist soils across the southern Great Plains resulting from a wet March–July 2007 had dried sufficiently during the warm, dry conditions of the first half of August so as to not produce a significant positive impact upon the reintensification process as compared to climatology. The individual positive contributions of the early TC rainfall (e.g., Figs. 4a,c) and along-track TC rainfall signals to the peak simulated intensity of the vortex are very weak in nature and likely statistically indistinguishable from one another. The nonlinearity of the impacts of these signals is apparent, however, when considering the combination of the seasonal and early TC rainfall signals. This combination results in a simulated vortex intensity just below that of the control simulation. This suggests that the early rainfall from TC Erin (2007) over Texas was a crucial contributor, with the aforementioned seasonal signal, to the final intensity of the simulated and presumably observed vortex.

Third, the addition of the along-track TC rainfall signal to either the seasonal or early TC rainfall signals produces a very minimal positive impact in terms of the simulated intensity of the vortex. In the aggregate, the addition of the along-track TC rainfall signal to any of the simulations (Early Rain, Seasonal, or Early+Seasonal) only results in a minimal positive impact upon the intensity of the simulated vortex. This suggests that the along-track TC rainfall signal, or that which the Emanuel et al. (2008) hypothesis suggests drives the overland reintensification of TCs over Australia, is not a significant contributor to the intensity of the simulated and observed vortices. More to the point, these findings suggest that the *specific* along-track rainfall signal described by Emanuel et al. (2008) does not significantly impact the intensity of the vortex *in this case*. This idea is extended upon within the discussion in section 5.

b. *Physical link between soil moisture and the reintensification process*

Focus now shifts to how soil moisture positively impacts the intensity of the simulated TC Erin (2007) vortex. During the daytime hours on 18 August 2007, greater soil moisture content leads to greater surface latent heat flux magnitudes (Fig. 11). The seasonal signal (e.g., Figs. 11a–d) contributes most strongly to surface latent heat flux values, particularly to the south and east of the simulated vortex. Favorable contributions to the surface latent heat flux magnitude from the early rainfall signal (cf. Figs. 11b and 11d) are noted across central Texas. Minimal differences between each simulation are observed near the simulated vortex itself. The net effect of the greater surface latent heat flux magnitudes is to reduce the surface Bowen ratio, or the ratio of the surface sensible to the surface latent heat flux. Over uniform soil types, Santanello et al. (2005) previously showed that this value is inversely correlated to soil moisture content, where greater soil moisture content results in reduced surface Bowen ratios via an increased

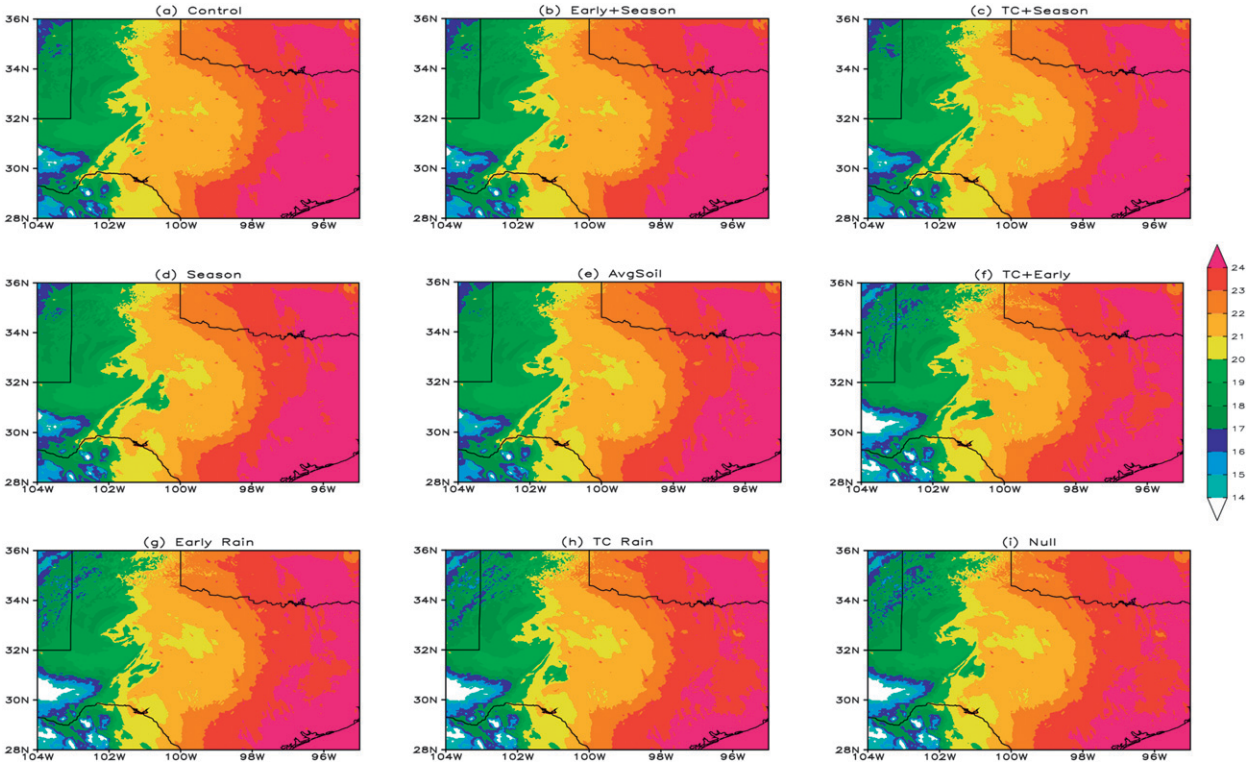

FIG. 16. As in Fig. 14, but valid at 1200 UTC 18 Aug 2007 and without the sounding locations displayed.

surface latent heat flux. A reduced surface Bowen ratio leads to reduced boundary layer mixing both near the vortex (Fig. 12) as well as in its outer inflow environment (Fig. 13), in turn resulting in a shallower boundary layer. A shallower boundary layer is generally less conducive to the deleterious effects of evaporationally driven cold pools upon the near-surface circulation. Variance of up to 50 hPa in the depth of the boundary layer is noted between the simulations within both regions.

In addition, the simulations with greater surface latent heat fluxes have greater moisture and instability, as reflected in Figs. 14 and 15. Specifically, 2-m dewpoint temperatures range from 1–2 K larger near the vortex to 3–4 K larger within the outer inflow region across central Texas in the simulations with moister soil conditions during the reintensification period (Fig. 14). Similarly, surface-based CAPE ranges from roughly 100 J kg^{-1} larger near the vortex to 500–1000 J kg^{-1} larger within the outer inflow region across central Texas in the simulations with moister soil conditions (Fig. 15). At earlier times (e.g., predawn on 18 August 2007) the differences in these fields between simulations are much smaller (e.g., <1 K in terms of 2-m dewpoint temperature; Fig. 16), suggesting that controls on daytime mixing within the boundary layer are the primary influences upon the differences in the specific thermodynamic fields shown in Figs. 14 and 15. Greater boundary layer moisture and instability may result in more robust convection (given an appreciable convective triggering mechanism) and accompanying latent heat release aloft.

Note that despite shallower and moister boundary layers within the stronger simulations, these simulations show minimal evidence of evaporation-driven surface cold pools, particularly near the vortex itself (Fig. 17). This allows for the maintenance of a convergent near-surface wind profile, thereby promoting rising motion over both convective and vortex scales within the vortex's environment in both the weakest and strongest simulations. In all, this suggests that soil moisture content does not significantly impact the potential for convectively generated cold pool development. We hypothesize that the lack of cold pools may be due to quasi-balanced lifting associated with the vortex itself, which could sufficiently moisten the atmospheric column and reduce evaporational cooling. Further analysis on the triggering, organization, and evolution of Erin's convection within each simulation is needed to test this hypothesis, however.

Differences in the intensity of the vortex at the surface may be highlighted in part by analyzing the vertical mass

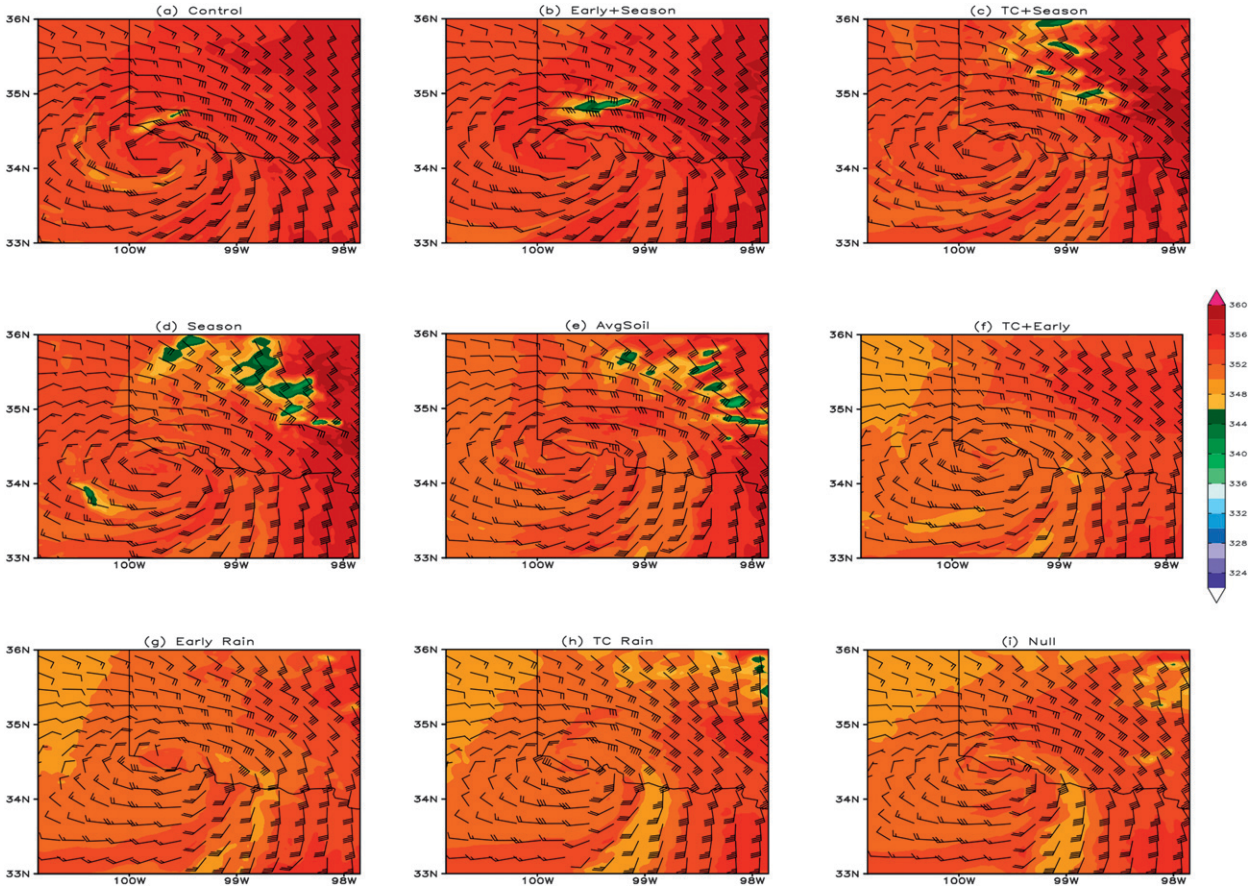

FIG. 17. As in Fig. 11, but for 925-hPa equivalent potential temperature (shaded; K) and 700-hPa wind field (barbs; kt) valid at 0600 UTC 19 Aug 2007.

flux, a reflection of the pressure-weighted vertical motion field (Davis and Galarneau 2009) and thus a reflection of the net impact of convective updrafts and downdrafts upon the transport of mass within the troposphere. The vertical mass flux is proportional to the diabatic heating rate (Ooyama 1971; Raymond and Sessions 2007) such that areas of positive vertical mass flux (and rising motion) are associated with areas of positive diabatic heating rates. Though much of the inferred diabatic heating is counterbalanced by adiabatic cooling in updrafts, when integrated both over the entire vortex and through time (to get an analog to net heating rather than heating rate), greater vertical mass fluxes may infer greater warm core development and subsequent vortex intensification via subsequent forcing on radial inflow and lower-tropospheric convergence (e.g., Eliassen 1951; Rogers and Fritsch 2001). In addition, positive vertical mass fluxes—or, more specifically, the vertical gradient thereof—also intrinsically reflect areas of greater amplification of cyclonic relative vorticity via stretching, reflecting a dynamical means by which greater vertical mass fluxes may positively impact vortex intensity.

The temporally and area-integrated vertical mass flux for each of the simulations conducted within this study is depicted in Fig. 18. The area integral computed here is done so within a $100 \times 100\ \text{km}^2$ box centered on the simulated vortex. Note that we do not observe any substantial differences in the horizontal scale of the vortex that could potentially bias these results in one direction (not shown). The net diabatic heating inferred by the temporally and area-integrated vertical mass flux is greater within the simulations featuring greater soil moisture content than in those with drier soils, particularly starting near the onset of the reintensification period. Differences in this net heating arise largely from the impacts of the previously shown differences in boundary layer moisture and instability (Figs. 11–15) upon convective intensity in an environment sufficiently moist so as to reduce convective downdraft and cold pool formation (Fig. 17). As a result, boundary layer radial inflow and convergence into the vortex is enhanced (Fig. 19) within the simulations

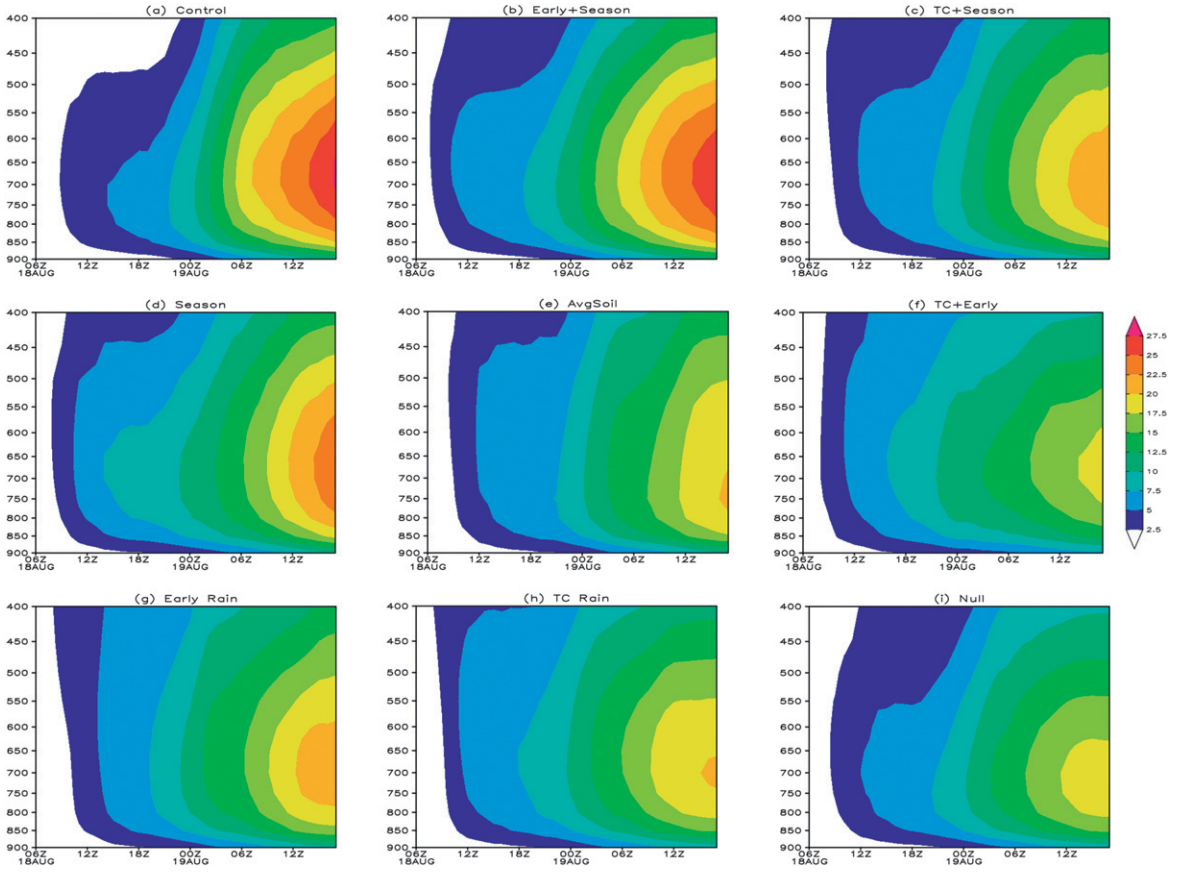

FIG. 18. Vertical profiles (between 900–400 hPa) of temporally and area-integrated (inside of a 100 × 100 km^2 box centered on the simulated vortex) vertical mass flux ($\times 10^{13}$ kg) between 0600 UTC 18 Aug 2007 and 1700 UTC 19 Aug 2007 from the (a) Control, (b) Early+Seasonal, (c) TC+Seasonal, (d) Seasonal, (e) Average Soil, (f) TC+Early, (g) Early Rain, (h) TC Rain, and (i) Null simulations. All fields are shaded per the color bar in (f).

exhibiting greater diabatic heating, contributing favorably to the intensification of the near-surface vortex.

Finally, it should be noted that an additional positive impact on the intensity of the vortex may come from the along-track surface latent heat fluxes during the reintensification period (Fig. 20). The presence of nonzero surface latent heat fluxes over land during this time in and of itself is notable as surface latent heat fluxes are typically near zero during the nighttime hours. Whether these nonzero surface latent heat fluxes are a reflection of the varying intensities of the vortex, varying soil conditions, some combination thereof, or something else altogether is uncertain. Nevertheless, peak surface latent heat flux magnitudes vary from approximately 150 W m^{-2} over a wide area with the most intense vortices and wettest soil conditions to approximately 75–100 W m^{-2} over a confined area with the weakest vortices and driest soil conditions. As noted previously (Emanuel et al. 2008; Montgomery et al. 2009), surface latent heat flux magnitudes of approximately 150 W m^{-2} appear to be sufficient to support vortices of strong tropical storm intensity. If TC Erin (2007) redeveloped as a TC, it stands to follow that in addition to the factors described above, reduced surface latent heat flux values along the track of the vortex would result in a weaker vortex. Further work into the energetics of Erin's reintensification is necessary, however, to quantify this statement.

5. Conclusions

In this work, the overland reintensification of TC Erin (2007) has been examined utilizing output from a suite of high-resolution convective-permitting WRF-ARW v3.1 mesoscale model simulations. High soil moisture content across much of Texas and Oklahoma (Fig. 3b) was shown to inhibit boundary layer mixing and lead to greater boundary layer moisture and instability. In a deep moist environment lacking significant convective downdrafts and surface cold pool formation, greater diabatic heating and subsequent warm core vortex development is

realized. The Emanuel et al. (2008) along-track TC rainfall feedback mechanism was shown to be of minimal importance to the evolution of the vortex. Rather, the final intensity of the simulated (and presumably observed) vortex appears to be closely linked to the maintenance of boundary layer moisture over preexisting near-climatological soil moisture content along the track of the vortex and well above climatological soil moisture content, as aided by the substantial contribution of Erin's rains on 16–17 August, along inflowing air parcels from the northwestern Gulf of Mexico through central Texas.

The simulated vortex exhibited a structure similar to that of developing TCs, including a warm-core structure with +2-K thermal anomaly aloft inside of the radius of maximum winds. This is similar to the structure inferred from observations by Monteverdi and Edwards (2010). Furthermore, the simulated vortex reintensified in an environment that was favorable for TC development. Notable among these factors is low vertical wind shear of approximately 5 m s^{-1} and a deep moist troposphere with total precipitable water values of 60–70 mm near and ahead of the vortex. From a classic perspective, the only negative factor for TC development with TC Erin on the morning of 19 August 2007 was the presence of the vortex over land.

Previous studies have shown that tropical cyclones can redevelop over land if the environmental conditions are favorable for such development to occur (Emanuel et al. 2008). Specifically, Emanuel et al. (2008) posed that redevelopment into a system of near-hurricane intensity is possible over land with surface latent heat flux values of approximately 150 W m^{-2}, similar to those observed near the vortex in the simulations conducted in this study. Similarly, Montgomery et al. (2009) posed that TC development over water can occur with similarly low surface latent heat flux magnitudes. They argue that though development is aided if surface latent heat flux magnitudes are larger than the so-called trade wind values of approximately 150 W m^{-2}, intense TCs may develop over water if surface latent heat flux feedbacks are capped at those values. In light of these two studies, the results presented in this work force us to reconsider the underlying surface conditions that permit TC development. At a basic level, TC development appears to be possible if the underlying surface has relatively high heat conductivity and is relatively moist (e.g., Shen et al. 2002; Tuleya 1994), thus permitting sufficiently high surface latent heat flux magnitudes. Obviously, warm waters represent the best example of such an underlying surface, but this work and that of Emanuel et al. (2008) highlight other surfaces permitting the same mode of development.

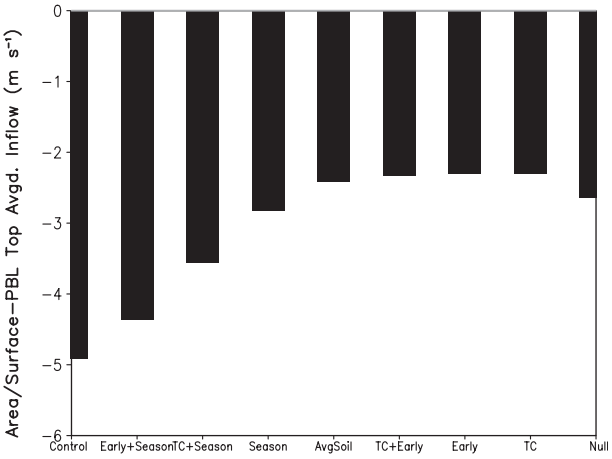

FIG. 19. Peak area-averaged (inside of a 100 × 100 km^2 box centered on the simulated vortex) surface to boundary layer top (as defined by the top of the mixed layer on the soundings in Fig. 12) layer mean radial inflow (m s^{-1}; negative values denote inflow) into the simulated Erin vortex from each of the simulations conducted in this study between 0000 and 1200 UTC 19 Aug 2007.

Despite their importance to the reintensification process, the favorable land surface feedbacks and environmental conditions detailed within this work are merely necessary but not sufficient conditions for vortex reintensification. In addition to these considerations, the development and organization of deep moist convection near the center of the vortex is necessary—and perhaps sufficient—for vortex reintensification to occur. It remains an open question as to which lifting mechanism(s), such as balanced lifting associated with the vortex in a vertically sheared environment (e.g., Trier and Davis 2002) and quasigeostrophic forcing for ascent associated with a weak transient upper-tropospheric trough north of Erin (e.g., Brennan et al. 2009), were most important to initiating and organizing convection about the center of the vortex. It also remains unclear as to why convectively generated cold pool activity was relatively minimal with this case. Furthermore, it remains to be quantified why the convective development and reorganization occurred during the nighttime hours, when surface latent heat fluxes were at a minimum and continental convection would tend to become elevated rather than surface based in nature. Future work will attempt to quantify these processes along with the forecastability inherent therein (e.g., Zhang and Sippel 2009; Snyder et al. 2011) for this case.

A number of unanswered questions remain related to sensitivities associated with the observed reintensification process. Why did Erin reintensify whereas other remnant tropical cyclones in the same region did not? From the perspective of the land surface, would Erin have reintensified as it did were it over cooler soils [e.g.,

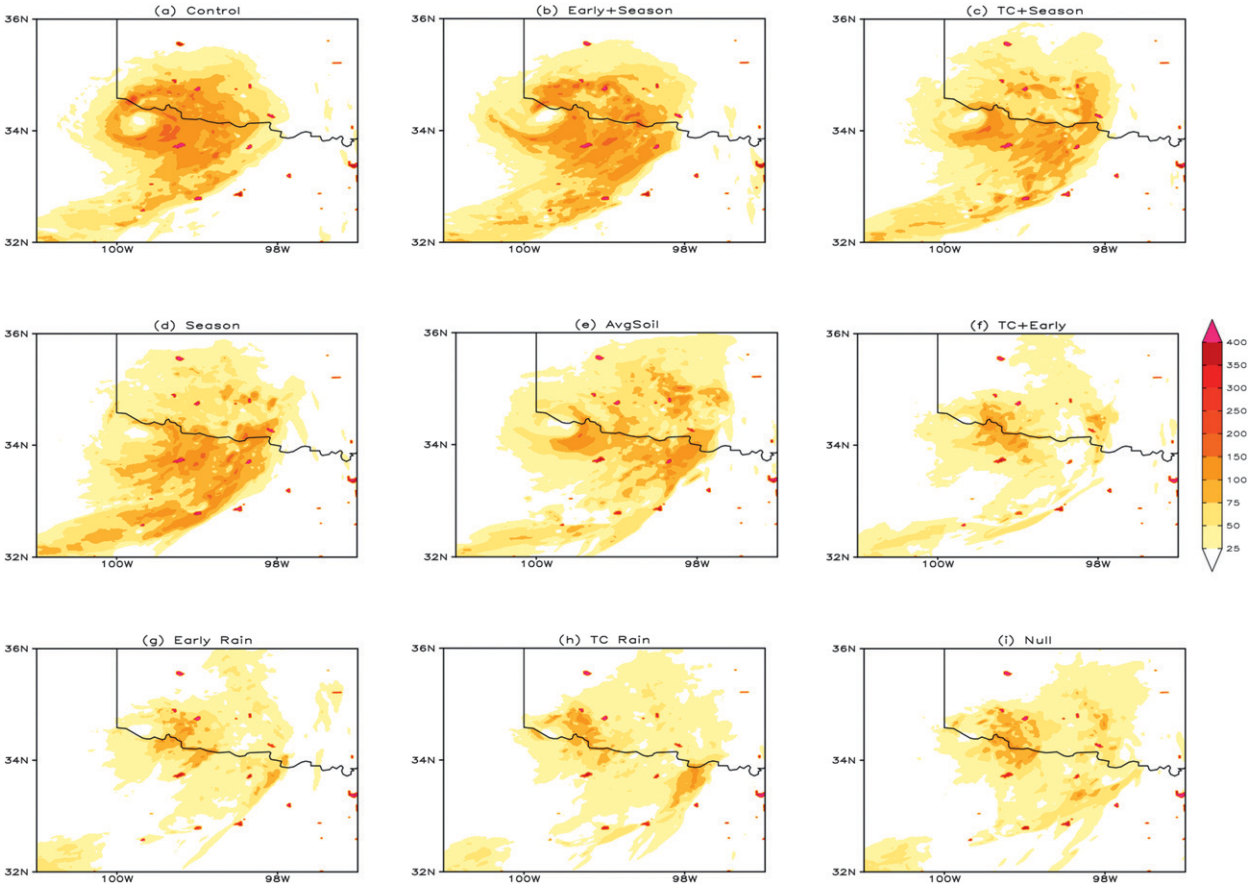

FIG. 20. As in Fig. 11, but valid at 0600 UTC 19 Aug 2007.

the sensitivity to soil temperature highlighted by Emanuel et al. (2008)]? Similarly, if the underlying soils were less sandy and thus had lesser heat conductivities than those over northern Texas and southern Oklahoma, how would the evolution have differed from that which was observed? Conversely, if the remnant Erin vortex traversed warm waters rather than wet land on 19 August 2007, would an even greater deepening have been observed? Each of these questions invites further study utilizing mesoscale model simulations and, in the aggregate, would provide new insights into the range of conditions under which tropical cyclones can evolve over land.

In addition, a full treatment of the dynamics and energetics of the reintensification process is necessary to conclusively determine whether Erin was a TC while over Oklahoma or not. Unresolved issues in this realm include, but are not limited to, the quantification of vorticity generation, merger, and axisymmetrization processes (e.g., Hendricks et al. 2004; Montgomery et al. 2006; Fang and Zhang 2010) and the possible contribution(s) of surface latent heat fluxes over land to the intensity of the vortex apart from the land surface feedback mechanisms discussed here. Future work will attempt to answer these questions and others.

Acknowledgments. Simulations performed in this study were conducted using the resources of the NCAR bluefire supercomputer. Level-II radar data depicted in Fig. 6 were obtained from the National Climatic Data Center and displayed using the GRLevel2 software package. The authors thank Lance Bosart (SUNY-Albany), Bob Hart (Florida State University), Eric Hendricks (Naval Research Laboratory), Ron McTaggart-Cowan (Environment Canada), David Nolan (University of Miami), Paul Reasor (NOAA/AOML/HRD), George Bryan, Chris Davis, Ethan Gutmann, Stan Trier, and Morris Weisman (all NCAR) for their insights, discussions, and critiques of this work. Comments from Jason Sippel (NASA) were of substantial benefit to the makeup and quality of this manuscript. The comments of two anonymous reviewers further improved this manuscript. The first author was supported by a UCAR/NCAR Advanced Study Program (ASP) Post-Doctoral Fellowship, the second author was supported by NSF Grant AGS-0954908, while the third

author was supported in part by a UCAR/NCAR ASP Graduate Visitor Program fellowship and NSF Grant ATM-0553017.

REFERENCES

Arndt, D. S., J. B. Basara, R. A. McPherson, B. G. Illston, G. D. McManus, and D. B. Demko, 2009: Observations of the overland reintensification of Tropical Storm Erin (2007). *Bull. Amer. Meteor. Soc.,* **90,** 1079–1093.

Bassill, N. P., and M. C. Morgan, 2006: The overland reintensification of Tropical Storm Danny (1997). Preprints, *27th Conf. on Hurricanes and Tropical Meteorology,* Monterey, CA, Amer. Meteor. Soc., 6A.6. [Available online at http://ams.confex.com/ams/pdfpapers/108676.pdf.]

Bosart, L. F., and G. M. Lackmann, 1995: Postlandfall tropical cyclone reintensification in a weakly baroclinic environment: A case study of Hurricane David (1979). *Mon. Wea. Rev.,* **123,** 3268–3291.

Brennan, M. J., R. D. Knabb, M. Mainelli, and T. B. Kimberlain, 2009: Atlantic hurricane season of 2007. *Mon. Wea. Rev.,* **137,** 4061–4088.

Chen, F., and J. Dudhia, 2001: Coupling an advanced land-surface/hydrology model with the Penn State–NCAR MM5 modeling system. Part I: Model description and implementation. *Mon. Wea. Rev.,* **129,** 569–585.

Chen, S.-H., and W.-Y. Sun, 2002: A one-dimensional time dependent cloud model. *J. Meteor. Soc. Japan,* **80,** 99–118.

Davis, C. A., and S. B. Trier, 2007: Mesoscale convective vortices observed during BAMEX. Part I: Kinematic and thermodynamic structure. *Mon. Wea. Rev.,* **135,** 2029–2049.

——, and T. J. Galarneau Jr., 2009: The vertical structure of mesoscale convective vortices. *J. Atmos. Sci.,* **66,** 686–704.

——, and Coauthors, 2008: Prediction of landfalling hurricanes with the Advanced Hurricane WRF model. *Mon. Wea. Rev.,* **136,** 1990–2005.

Done, J., C. A. Davis, and M. Weisman, 2004: The next generation of NWP: Explicit forecasts of convection using the Weather Research and Forecasting (WRF) model. *Atmos. Sci. Lett.,* **5,** 110–117.

Dudhia, J., 1989: Numerical study of convection observed during the winter monsoon experiment using a mesoscale two-dimensional model. *J. Atmos. Sci.,* **46,** 3077–3107.

Eliassen, A., 1951: Slow thermally or frictionally controlled meridional circulation in a circular vortex. *Astrophys. Norv.,* **5,** 19–60.

Emanuel, K., cited 2008: Non-baroclinic inland rejuvenation of tropical cyclones. [Available online at http://www.meteo.mcgill.ca/cyclone/lib/exe/fetch.php?id=start&cache=cache&media=wed2030.ppt.]

——, J. Callaghan, and P. Otto, 2008: A hypothesis for the redevelopment of warm core cyclones over northern Australia. *Mon. Wea. Rev.,* **136,** 3863–3872.

Environmental Modeling Center, 2003: The GFS Atmospheric Model. NCEP Office Note 442, 14 pp.

Fang, J., and F. Zhang, 2010: Initial development and genesis of Hurricane Dolly (2008). *J. Atmos. Sci.,* **67,** 655–672.

Fritsch, J. M., J. D. Murphy, and J. S. Kain, 1994: Warm core vortex amplification over land. *J. Atmos. Sci.,* **51,** 1780–1807.

Galarneau, T. J., Jr., L. F. Bosart, and R. S. Schumacher, 2010: Predecessor rain events ahead of tropical cyclones. *Mon. Wea. Rev.,* **138,** 3272–3297.

Geo4Va, cited 2011: Seasonal temperature cycles. [Available online at http://www.geo4va.vt.edu/A1/A1.htm.]

Gray, W. M., 1968: Global view of the origin of tropical disturbances and storms. *Mon. Wea. Rev.,* **96,** 669–700.

Hanley, D., J. Molinari, and D. Keyser, 2001: A composite study of the interactions between tropical cyclones and upper-tropospheric troughs. *Mon. Wea. Rev.,* **129,** 2570–2584.

Hendricks, E. A., M. T. Montgomery, and C. A. Davis, 2004: The role of ''vortical'' hot towers in the formation of Tropical Cyclone Diana (1984). *J. Atmos. Sci.,* **61,** 1209–1232.

Hong, S.-Y., Y. Noh, and J. Dudhia, 2006: A new vertical diffusion package with an explicit treatment of entrainment processes. *Mon. Wea. Rev.,* **134,** 2318–2341.

Koster, R. D., Z. Guo, R. Yang, P. A. Dirmeyer, K. Mitchell, and M. J. Puma, 2009: On the nature of soil moisture in land surface models. *J. Climate,* **22,** 4322–4335.

Menard, R. D., and J. M. Fritsch, 1989: A mesoscale convective complex–generated inertially stable warm core vortex. *Mon. Wea. Rev.,* **117,** 1237–1261.

Mesinger, F., and Coauthors, 2006: North American Regional Reanalysis. *Bull. Amer. Meteor. Soc.,* **87,** 343–360.

Mlawer, E. J., S. J. Taubman, P. D. Brown, M. J. Iacono, and S. A. Clough, 1997: Radiative transfer for inhomogeneous atmosphere: RRTM, a validated correlated-k model for the longwave. *J. Geophys. Res.,* **102** (D14), 16 663–16 682.

Monteverdi, J. P., and R. Edwards, 2010: The redevelopment of a warm-core structure in Erin: A case of inland tropical storm formation. *Electron. J. Severe Storms Meteor.,* **5** (6), 1–18.

Montgomery, M. T., M. E. Nicholls, T. A. Cram, and A. B. Saunders, 2006: A vortical hot tower route to tropical cyclogenesis. *J. Atmos. Sci.,* **63,** 355–386.

——, V. S. Nguyen, J. Persing, and R. K. Smith, 2009: Do tropical cyclones intensify by WISHE? *Quart. J. Roy. Meteor. Soc.,* **135,** 1697–1714.

Ooyama, K., 1971: A theory of parameterization of cumulus convection. *J. Meteor. Soc. Japan,* **49,** 744–756.

Raymond, D. J., and S. Sessions, 2007: Evolution of convection during tropical cyclogenesis. *Geophys. Res. Lett.,* **34,** L06811, doi:10.1029/2006GL028607.

Rogers, R. F., and J. M. Fritsch, 2001: Surface cyclogenesis from convectively-driven amplification of midlevel mesoscale convective vortices. *Mon. Wea. Rev.,* **129,** 605–637.

Rotunno, R., and K. Emanuel, 1987: An air-sea interaction theory for tropical cyclones. Part II: Evolutionary study using a nonhydrostatic axisymmetric numerical model. *J. Atmos. Sci.,* **44,** 542–561.

Santanello, J. A., Jr., M. A. Friedl, and W. P. Kustas, 2005: An empirical investigation of convective planetary boundary layer evolution and its relationship with the land surface. *J. Appl. Meteor.,* **44,** 917–932.

Schumacher, R. S., and R. H. Johnson, 2009: Quasi-stationary, extreme-rain-producing convective systems associated with midlevel cyclonic circulations. *Wea. Forecasting,* **24,** 555–574.

——, T. J. Galarneau, and L. F. Bosart, 2011: Distant effects of a recurving tropical cyclone on rainfall in a midlatitude convective system: A high-impact predecessor rain event. *Mon. Wea. Rev.,* **139,** 650–667.

Shen, W., I. Ginis, and R. E. Tuleya, 2002: A numerical investigation of land surface water on landfalling hurricanes. *J. Atmos. Sci.,* **59,** 789–802.

Skamarock, W. C., and Coauthors, 2008: A description of the Advanced Research WRF version 3. NCAR Tech. Note NCAR/TN-475+STR, 125 pp.

Snyder, A., Z. Pu, and C. A. Reynolds, 2011: Impact of stochastic convection on ensemble forecasts of tropical cyclone development. *Mon. Wea. Rev.,* **139,** 620–626.

Trier, S. B., and C. A. Davis, 2002: Influence of balanced motions on heavy precipitation within a long-lived convectively generated vortex. *Mon. Wea. Rev.,* **130,** 877–899.

——, ——, and J. D. Tuttle, 2000: Long-lived mesoconvective vortices and their environment. Part I: Observations from the central United States during the 1998 warm season. *Mon. Wea. Rev.,* **128,** 3376–3395.

——, F. Chen, and K. W. Manning, 2004: A study of convection initiation in a mesoscale model using high-resolution land surface initial conditions. *Mon. Wea. Rev.,* **132,** 2954–2976.

Tuleya, R. E., 1994: Tropical storm development and decay: Sensitivity to surface boundary conditions. *Mon. Wea. Rev.,* **122,** 291–304.

Weisman, M. L., C. A. Davis, W. Wang, K. W. Manning, and J. B. Klemp, 2008: Experiences with 0-36-h explicit convective forecasts with the WRF-ARW model. *Wea. Forecasting,* **23,** 407–437.

Yu, C.-K., B. J.-D. Jou, and B. F. Smull, 1999: Formative stage of a long-lived mesoscale vortex observed by airborne Doppler radar. *Mon. Wea. Rev.,* **127,** 838–857.

Zhang, F., and J. A. Sippel, 2009: Effects of moist convection on hurricane predictability. *J. Atmos. Sci.,* **66,** 1944–1961.